



# Polymer-Modified Oligonucleotide Sequences: Towards Biologically Active Self-Assembled Interfaces

Inauguraldissertation  
Zur  
Erlangung der Würde eines Doktors der Philosophie

Vorgelegt der  
Philosophisch-Naturwissenschaftlichen Fakultät  
Der Universität Basel

Von  
**Francisco José Teixeira Jr.**  
Aus Caruaru, PE, Brasilien

Basel 2009

Original document stored on the publication server of the University of Basel  
[edoc.unibas.ch](http://edoc.unibas.ch)



This work is licenced under the agreement „Attribution Non-Commercial No Derivatives – 2.5  
Switzerland“. The complete text may be viewed here:  
[creativecommons.org/licenses/by-nc-nd/2.5/ch/deed.en](http://creativecommons.org/licenses/by-nc-nd/2.5/ch/deed.en)

Genehmigt von der Philosophisch-Naturwissenschaftlichen Fakultät  
Auf Antrag von

Dr. Corinne Vebert-Nardin  
Prof. Dr. Wolfgang Meier  
Dr. Helmut Schlaad

Basel, den 26 Mai 2009

Prof. Dr. Eberhard Parlow  
Dekan

I dedicate this thesis to Polyana Augusta Bastos Teixeira, my dearest wife, who has always stayed by my side, motivating me and helping me follow my dreams. For her love, patience, support and trust in me I will always be grateful.

*“Life is not easy for any of us. But what of that? We must have perseverance and above all confidence in ourselves. We must believe that we are gifted for something, and that this thing, at whatever cost, must be attained.”*

*Marie Curie, physicist, 1867-1934*

*“Nothing in this world can take the place of persistence. Talent will not; nothing is more common than unsuccessful people with talent. Genius will not; unrewarded genius is almost a proverb. Education will not; the world is full of educated derelicts. Persistence and determination alone are omnipotent. The slogan ‘press on’ has solved and always will solve the problems of the human race.”*

*Calvin Coolidge, 30<sup>th</sup> US President, 1872-1933*

## Acknowledgements

Now that we come to the end of this work, there are a number of people to whom I should and would like to say thank you:

Firstly I would like to thank God, who has always watched over me. He showed me the path even in the moments when everything seemed hopeless.

For the love and support of my family in Brazil (my parents Francisco and Rosário, my aunt Carminha, my brother Fábio, my sister Flávia and my grandparents Sabino, *in memorian* and Dulce, *in memorian*) I can never be thankful enough. Their sacrifice is the reason I was ever able to come this far. I miss them every day.

For the confidence of Dr. Corinne Vebert-Nardin I will be forever grateful. She entrusted me with her research and gave me the opportunity to develop my skills as a chemist and a scientist. This is the result of that trust and I am proud of it.

To Prof. Dr. Wolfgang Meier for giving me the opportunity to develop this research project in the research facilities of his group. To my friends and colleagues during this PhD work, Julia, Kelnner and Nicolas, and to the whole Meier group, with whom I had the honor of sharing this experience.

To all of my friends, who supported me in my journey, even if only from far away, and to all of those who contributed in any way for this realization of this work.

To the Swiss National Fund, SNF for the financial support of this project.

## Table of Contents

Acknowledgements	1
Table of Contents	2
1. Introduction	4
1.1. Polymers and Copolymers	5
1.2. Oligonucleotides and Oligonucleotide-Based Materials	6
1.3. Scope of the Thesis	7
1.4. References	8
2. Synthesis	12
2.1. Oligonucleotides	12
2.2. Poly(butadiene)	17
2.2.1. End Group Modification	18
2.2.2. Primary Amino End-Functionalized One-Pot Synthesis	21
2.3. Polymer-Modified Oligonucleotides	23
2.3.1. Solid Phase Chemistry	23
2.3.2. Heterogeneous Biphasic Chemistry	30
2.4. References	35
3. Self-Assembly	37
3.1. Block Copolymers	37
3.2. Charged Block Copolymers	40
3.3. Polymer-Modified Oligonucleotides	41
3.3.1. Size Determination	43
3.3.2. Morphological Studies	48
3.4. References	55
4. Biological Activity	58
4.1. Hybridization	58
4.1.1. Oligonucleotide Configurational Analyses	60

4.1.2. Preliminary Hybridization Studies _____	61
4.2. Preliminary Biological Assays _____	65
4.2.1. Cytotoxicity studies _____	66
4.2.2. Internalization studies _____	68
4.3. References _____	70
5. Conclusion and Outlook _____	72
6. Materials and Methods _____	75
Curriculum Vitae _____	79

## Chapter 1: Introduction

The evolution of Science is quite amazing. Natural phenomena have always stirred the curiosity of human kind and, because of that, man has always tried to understand, quantify, mimic and otherwise take advantage of the possibilities offered by Nature. In this thirst for knowledge and understanding, science has flourished, although not without its mistakes and misconceptions, but always trying to better itself and improve the quality of life of Humanity.

The development and use of new technologies and equipments has taken society to new levels of prosperity, in which science has a deeper understanding of the mechanisms that govern Life and the Universe around us. But in order to continue thriving, Science is always faced with new challenges that defy our current ability and knowledge, motivating invention and the discovery of new technologies to overcome the barriers and difficulties in the way.

One of the challenges we have been faced with since the late XX century in the field of biology and nanotechnology is the need for smart materials, able to mimic the outstanding properties of biological molecules, but yet having excelling properties when compared to the latter, coupling higher stability and functionality. For instance, the technology of drug delivery requires carrier systems to be not only stable *in vivo*, but also able to recognize specific targets in the organism<sup>1-3</sup>.

In pursue of these smart materials, organic synthetic chemists develop compounds such as drugs capable of copying the activity and specificity of biological molecules, becoming ever more efficient with the passing years<sup>4-6</sup>. These drugs are capable of either activating certain pathways in metabolic mechanisms<sup>7</sup> or acting as inhibitors in others<sup>8</sup>.

We go even further, using natural molecules to mimic Nature itself: polypeptide-based polymers<sup>9-11</sup> and DNA-based macromolecules, which take advantage of the highly specific properties of these natural polymers in a wide range of applications<sup>12-17</sup>.



## 1.1. Polymers and Copolymers

Among all these materials, copolymers are macromolecules of special interest in several areas of natural sciences, mainly because of their versatile chemistry and hierarchical, stimuli responsive organization at several length scales<sup>9-11,16,17,18-22</sup>.

Block copolymers are macromolecules composed by two or more homopolymers covalently linked<sup>23</sup>. These copolymers are classified based on the arrangement of the homopolymer blocks, achieving various architectures (figure 1.1).

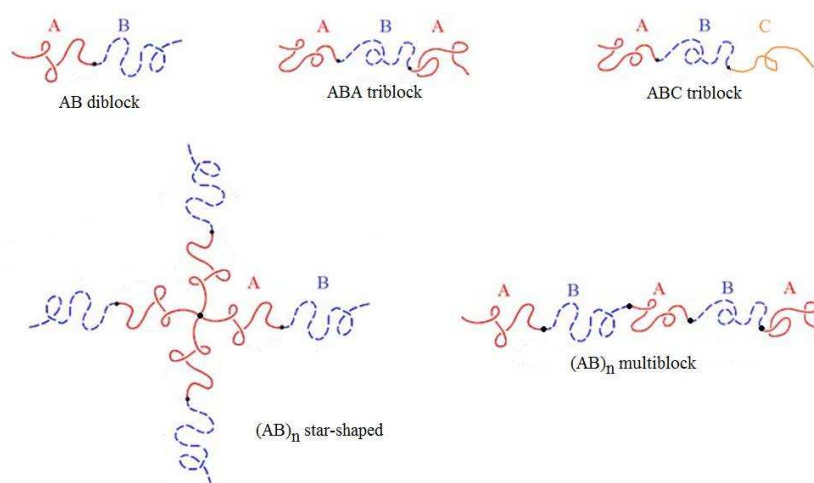


Figure 1.1. Common architectures of synthetic block copolymers.

Amphiphilic diblock and triblock copolymers are especially attractive to the field of drug delivery due to their ability to self-assemble (to be further discussed in chapter 3: Self-Assembly). Self-assembled morphologies, which organize into a membrane-like structure, can be viewed as analogous to the biological membranes<sup>24,25</sup>. The interest arises from the fact that, even though many of the state of the art drugs are very active, such as doxorubicin and indomethacin (used against cancer), they do not have sufficient half-life time in the organism, needing therefore to be incorporated in a carrier<sup>1-3,26-29</sup>.

Other interesting application of block copolymers is the design of solid-supported membranes<sup>30,31</sup>. The copolymers can either be tethered to surfaces, serving as model membranes to understand the physical and chemical characteristics of membranes and membrane function<sup>32</sup>, or arrayed onto surfaces in their self-assembled form, in order to study, for instance, the effects of the

introduction of these structures on the adhesion of cells and bacteria onto surfaces<sup>33,34</sup>.

Independent of the application, the need for materials with higher sensitivity to environmental stimuli and biological activity leads scientists to develop an increasing number of compounds based on naturally active molecules. Among the new materials, those employing oligonucleotides are a novel, attractive and challenging group.

## 1.2. Oligonucleotides<sup>35</sup> and Oligonucleotide-Based Materials

Nucleotides are the monomers, i.e. the building blocks of the deoxyribonucleic acid, DNA and ribonucleic acid, RNA. These natural polymers code the genetic information of all living creatures and are composed by five different nucleobases: adenine (A), thymine (T), guanine (G), cytosine (C) and uracil (U), being the latter present in RNA only, in substitution of thymine.

The structures that result from the combination of these nucleobases with a sugar (the pentose 2-deoxyribose for DNA and ribose for RNA) are called nucleosides. If a nucleoside is coupled to a monophosphate group it is referred to as deoxynucleotide and nucleotide, respectively.

In order to simplify the nomenclature of these compounds and considering that this research work was based on the study of DNA related structures, we will not refer to RNA from this point on and the deoxynucleotides will be simply called nucleotides. The structures of the nucleotides that compose DNA are shown below in figure 1.2.

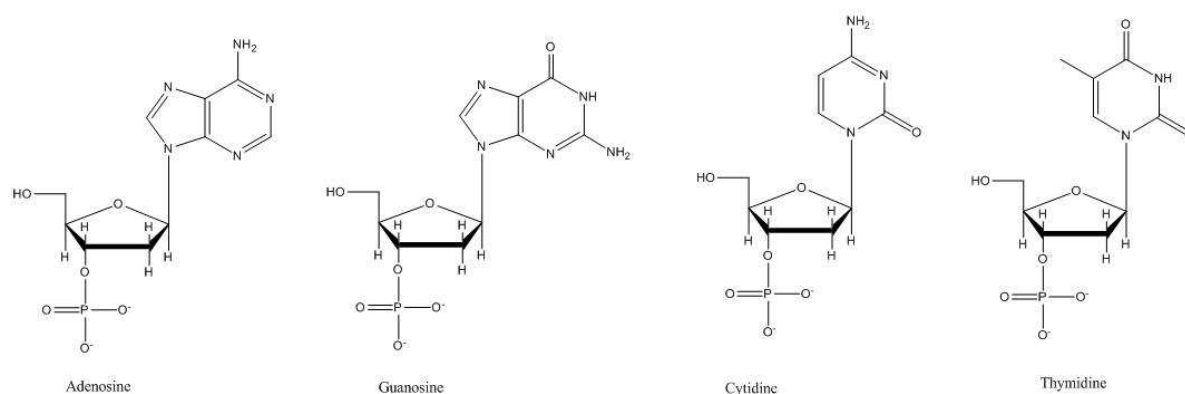


Figure 1.2. Nucleotides that compose the DNA strands.

Oligonucleotides are short sequences of nucleotides in which the order of the monomers in the strand is predetermined and can be synthesized in the laboratory with a very high degree of control. This is one of the reasons why their use in scientific applications have been increasing at growing rates for the past years.

The DNA chip technology<sup>36</sup>, the oligonucleotide mediated cell adhesion<sup>37</sup>, the use as scaffolds for the synthesis of conductive polymers<sup>38</sup> and the use as hydrophilic block in amphiphilic copolymers are but some of the applications of oligonucleotides.

### 1.3. Scope of the Thesis

The *status quo* of Science, its willingness to evolve and the ever increasing need for more specific, responsive materials is the driving force that inspires the development of material sciences. Oligonucleotides, on the other hand, are a class of biologically active material that has drawn much attention in recent years.

Taking all this facts in consideration, this research work aims to contribute, even if only modestly, to the advancement of smart, biologically active materials and to the improvement of the available technology of drug delivery system. In order to achieve this purpose, new amphiphilic copolymeric systems based on oligonucleotides were designed.

In order to make these systems accessible, simpler and more effective routes for the synthesis of the oligonucleotide-based copolymers should be developed by considering the fundamental chemical and physical properties of the blocks involved. As a consequence, two different synthetic approaches were developed.

After synthesis of these polymer-modified oligonucleotides, the study of their self-assembly in aqueous solution was to be performed. These studies had the objective of understanding the influence of the oligonucleotides on the morphological properties of the self-assembled copolymers and responsiveness of these structures to environmental stimuli.

Finally, preliminary studies regarding the polymer-modified oligonucleotides to specifically interact with their complementary nucleotide strands were to be carried out. These studies intended to determine whether they were capable of undergoing specific recognition mechanisms mediated by nucleotide sequences.

#### 1.4. References

1. Di Stefano, A.; Sozio, P.; Iannitelli, A.; Cerasa, L.S. New drug delivery strategies for improved Parkinson's disease therapy. *Expert Opin. Drug Deliv.* **2009**, *6*, 389-404.
2. Hammarlund-Udenaes, M.; Bredberg, U.; Friden, M. Methodologies to assess brain drug delivery in lead optimization. *Curr. Top. Med. Chem.* **2009**, *9*, 148-162.
3. Smith, B.; Uhl, K. Drug Delivery in the Twenty-First Century: A New Paradigm. *Clin. Pharmacol. Ther.* **2009**, *85*, 451-455.
4. Sugiyama, S.; Miki, T.; Nishikawa, H. Curative drug for neurodegenerative diseases. *U.S. Pat. Appl. Publ.* **2009**, 5pp.
5. Maya, J.D.; Cassels, B.K.; Iturriaga-Vasquez, P.; Ferreira, J.; Faundez, M.; Galanti, N.; Ferreira, A.; Morello, A. Mode of action of natural and synthetic drugs against *Trypanosoma cruzi* and their interaction with the mammalian host. *Comp. Biochem. Physiol., Part A Mol. Integr. Physiol.* **2007**, *146A*, 601-620.
6. Mimeault, M.; Batra, S.K. Recent advances in the development of novel anti-cancer drugs targeting cancer stem/progenitor cells. *Drug Dev. Res.* **2008**, *69*, 415-430.
7. Andreas, K.; Haeupl, T.; Luebke, C.; Ringe, J.; Morawietz, L.; Wachtel, A.; Sittinger, M.; Kaps, C. Antirheumatic drug response signatures in human chondrocytes: potential molecular targets to stimulate cartilage regeneration. *Arthritis Res. Ther.* **2009**, *11*, R15.
8. Araujo, E.P.; Carnevalheira, J. B.; Velloso, L.A. Disruption of metabolic pathways - perspectives for the treatment of cancer. *Curr. Cancer Drug Targets* **2006**, *6*, 77-87.
9. Boerner, H. G.; Schlaad, H. Bioinspired functional block copolymers. *Soft Matter* **2007**, *3*, 394-408.
10. Agut, W.; Taton, D.; Lecommandoux, S. A Versatile Synthetic Approach to Polypeptide Based Rod-Coil Block Copolymers by Click Chemistry. *Macromolecules* **2007**, *40*, 5653-5661.
11. Deming, Timothy J. Polypeptide and polypeptide hybrid copolymer synthesis via NCA polymerization. *Adv. Polymer Sci.* **2006**, *202* (*Peptide Hybrid Polymers*), 1-18.

12. Diculescu, V.C.; Paquim, A.-M.C.; Brett, A.M.O. Electrochemical DNA sensors for detection of DNA damage. *Sensors* **2005**, *5*, 377-393.
13. Warner, M.G.; Hutchison, J. E. Linear assemblies of nanoparticles electrostatically organized on DNA scaffolds. *Nat. Mater.* **2003**, *2*, 272-277.
14. Bier, Frank F.; von Nickisch-Roseneck, Markus; Ehrentreich-Foerster, Eva; Reiss, Edda; Henkel, Joerg; Strehlow, Rothin; Andresen, Dennie. DNA microarrays. *Adv. Biochem. Eng. Biotechnol.* **2008**, *109* (*Biosensing for the 21st Century*), 433-453.
15. Huang, Y.C.; Ge, B.; Sen, D.; Yu, H.-Z. Immobilized DNA Switches as Electronic Sensors for Picomolar Detection of Plasma Proteins. *J. Am. Chem.* **2008**, *130*, 8023-8029.
16. Alemdaroglu, F.E.; Herrmann, A. DNA meets synthetic polymers - highly versatile hybrid materials. *Org. Biomol. Chem.* **2007**, *5*, 1311-1320.
17. Teixeira Jr., F.; Rigler, P.; Vebert-Nardin, C. Nucleo-copolymers: Oligonucleotide-based amphiphilic diblock copolymers. *Chem. Comm.* **2007**, *11*, 1130-1132.
18. Vandermeulen, G.W.M.; Klok, H.-A. Synthesis of poly(ethylene glycol)-B-peptide diblock copolymers – towards stimuli-sensitive self-assembled materials. *Polymer Prepr.* **2001**, *42*, 84-85.
19. Schacher, F.; Muellner, M.; Schmalz, H.; Mueller, A.H.E. New block copolymers with poly(N,N-dimethylaminoethyl methacrylate) as a double stimuli-responsive block. *Macromol. Chem. Phys.* **2009**, *210*, 256-262.
20. Checot, F.; Rodriguez-Hernandez, J.; Gnanou, Y.; Lecommandoux, S. pH-responsive micelles and vesicles nanocapsules based on polypeptide diblock copolymers. *Biomol. Eng.* **2007**, *24*, 81-85.
21. Ma, Y.; Tang, Y.; Billingham, N.C.; Armes, S.P.; Lewis, A.L. Synthesis of biocompatible, stimuli-responsive, physical gels based on ABA triblock copolymers. *Biomacromolecules* **2003**, *4*, 864-868.
22. Onaca, O.; Enea, R.; Hughes, D.W.; Meier, W. Stimuli-responsive polymersomes as nanocarriers for drug and gene delivery. *Macromol. Biosci.* **2009**, *9*, 129-139.
23. IUPAC. Glossary of Basic Terms in Polymer Science. *Pure Appl. Chem.* **1996**, *68*, 2287-2311.
24. Mecke, A.; Dittrich, C.; Meier, W. Biomimetic membranes designed from amphiphilic block copolymers. *Soft Matter* **2006**, *2*, 751-759.

25. Choi, H.-J.; Brooks, E.; Montemagno, C.D. Synthesis and characterization of nanoscale biomimetic polymer vesicles and polymer membranes for bioelectronic applications. *Nanotechnology* **2005**, *16*, S143-S149.
26. Yokoyama M.; Kwon G.S.; Okano T.; Sakurai Y.; Seto T.; Kataoka K. Preparation of micelle-forming polymer–drug conjugates. *Bioconjug. Chem.* **1992**, *3*, 295-301.
27. Rapoport, N. Combined Cancer Therapy by Micellar-Encapsulated Drug and Ultrasound. *Int. J. Pharm.* **2004**, *277*, 155-162.
28. Lin, W.J.; Juang L.W.; Lin, C.C. Stability and release performance of a series of pegylated copolymeric micelles. *Pharm. Res.* **2003**, *20*, 668-673.
29. Djordjevic, J.; Barch, M.; Uhrich, K.E. Polymeric micelles based on amphiphilic scorpion-like macromolecules: novel carriers for water-insoluble drugs. *Pharm. Res.* **2005**, *22*, 24-32.
30. Rakhmatullina, E.; Manton, A.; Burgi, T.; Malinova, V.; Meier, W. Solid-supported amphiphilic triblock copolymer membranes grafted from gold surface. *J. Polym. Sci. [A1]* **2008**, *47*, 1-13.
31. Rakhmatullina, E.; Braun, T.; Chami, M.; Malinova, V.; Meier, W. Self-Organization Behavior of Methacrylate-Based Amphiphilic Di- and Triblock Copolymers. *Langmuir* **2007**, *23*, 12371-12379.
32. Tanaka, M.; Sackmann, E. Supported Lipid Membranes as Cell/Tissue Surface Models. *Nature* **2005**, *437*, 656-663.
33. Cottenye, N.; Teixeira Jr., F.; Ponche, A.; Reiter, G.; Anselme, K.; Meier, W.; Ploux, L.; Vebert-Nardin, C. Oligonucleotide nanostructured surfaces: Effect on *Escherichia coli* curli expression. *Macromol. Biosci.* **2008**, *8*, 1161-1172.
34. Nejadnik, M.R.; van der Mei, H.C.; Norde, W.; Busscher, H.J. Bacterial adhesion and growth on a polymer brush-coating. *Biomaterials* **2008**, *29*, 4117-4121.
35. Blackburn, G.M. DNA and RNA structure. In *Nucleic Acids in Chemistry and Biology*, 2<sup>nd</sup> Edition; Blackburn, G.M., Gait, M.J., Eds.; Oxford University Press: New York, NY, USA, 1996.
36. Dandy, David S.; Wu, Peng; Grainger, David W. Array feature size influences nucleic acid surface capture in DNA microarrays. *PNAS* **2007**, *104*, 8223-8228.
37. Chandra, R.A.; Douglas, E.S.; Mathies, R.A.; Bertozzi, C.R.; Francis, M.B. Programmable Cell Adhesion Encoded by DNA Hybridization. *Angew. Chem. Int. Ed. Engl.* **2006**, *45*, 896-901.

38. Datta, B.; Schuster, G.B.; McCook, A.; Harvey, S.C.; Zakrzewska, K. DNA-Directed Assembly of Polyanilines: Modified Cytosine Nucleotides Transfer Sequence Programmability to a Conjoined Polymer. *J. Am. Chem. Soc.* **2006**, *128*, 14428-14429.

## Chapter 2: Synthesis

The development of the concepts involved in the synthesis of the nucleo-copolymers is directly related to the synthetic techniques used in the production of both its composing blocks: oligonucleotides (hydrophilic) and poly(butadiene) (hydrophobic) and their own chemical and physical-chemical properties. The particularities of the synthesis of the above mentioned materials, in particular the oligonucleotides, were of great importance in defining what sort of chemical route was to be applied. Hence, in order to clarify the synthetic choices made regarding the chemistry of the nucleo-copolymers, the synthesis of each of their building blocks will be discussed.

### 2.1. Oligonucleotides

The chemical synthesis of nucleic acids can be performed through a couple of different techniques, which will affect the properties of the product obtained. If the objective is to synthesize oligonucleotides, as in our case, the most suitable technique is the solid phase phosphoramidite synthesis. The standard synthetic method<sup>1,2</sup> involves the stepwise reaction and addition of a nucleotide derivative (phosphoramidite) to a nucleoside residue (in the first step) or to a nucleotide sequence already linked to the insoluble solid support, leading to the assembly of the oligonucleotides.

The solid-phase synthesis of oligonucleotides is generally performed onto a controlled pore glass (CPG) support, for the rigidity and non-swellability of the beads, as well as the inertness to all the reactants involved. The most used bead porosities are 500 and 1000 Å, being the latter more common for the synthesis of oligonucleotides bearing more than 80 residues.

The preparation of the beads usually involves the functionalization with a long spacer bearing an amine termination. The loading of this group onto the CPG is kept in the range of 10 to 50  $\mu\text{mol.g}^{-1}$  in order to avoid steric effects between the oligonucleotide chains, during the synthesis<sup>1</sup>. High load supports, carrying about 2.5 times the loading of normal CPGs (80-130  $\mu\text{mol.g}^{-1}$ ), already exist, though these



should not be used in the synthesis of sequences containing more than 40 nucleotides<sup>3</sup>.

The first species that is coupled to the support through the reaction of its 3'-succinate derivative with the amino groups present on the support is a deoxynucleoside. It is, thus, important to observe the fact that this synthesis will always link the 3'-end of the phosphoramidite to the 5'-end of the sequence onto the CPG. Therefore, the deoxynucleoside bound to the resin in the first step will be the 3'-terminus of the final nucleotide sequence.

To ensure high performance in the custom synthesis of oligonucleotides, the CPG beads are provided already functionalized with the oligonucleosides and appropriately end-capped, in order to avoid 3'-degenerated sequences, and packed into columns especially designed for the synthesis of oligonucleotides that can be loaded in the range of 40 nmoles to 15  $\mu$ moles. The syntheses are performed through the injection of solvents and reagents in a given order, normally using a DNA synthesizer.

The steps involved in the synthesis of any given nucleotide sequence on solid support by phosphoramidite chemistry are the following:

1 – Removal of the dimethoxytrityl protecting groups (detritylation) from the 5'-terminus of the nucleoside. The detritylation is achieved by the use of di- or trichloroacetic acid (DCA/TCA) in dichloromethane (DCM). As the dimethoxytrityl cation yields a solution of strong orange coloration, this step is used to quantify the *coupling efficiency* of the reaction by comparison with the previous cycle.

2 – Activation of the phosphoramidite by mixing with tetrazole in dry acetonitrile. The tetrazole activates the phosphoramidite by protonation of the tertiary nitrogen group.

3 – Addition and reaction of the activated phosphoramidite to the deprotected nucleotide sequence. The coupling occurs via a nucleophilic attack by the free 5'-hydroxyl group on the 3'-phosphorous group of the incoming activated monomer. The yield of the coupling step is generally close to 98%.

4 – Oxidation of the intermediary phosphite with iodine ( $I_2$ ) and water to obtain a phosphotriester. Pyridine or 2,6-lutidine is used to neutralize the hydrogen iodide (HI) formed.

5 – End-capping of the non-reacted chains in order to avoid the growth of faulty sequences. This is obtained by the coupling of unreacted sequences with an

appropriate species, such as an activated acetylating agent, from the mixing of an acidic anhydride and N-methylimidazole, or a phosphoramidite derivative, such as diethylene glycol monoethyl ether phosphoramidite, UniCap<sup>4</sup>.

This cycle is repeated for every phosphoramidite that is added to the growing chains on the support, thus increasing the length of the oligonucleotides (figure 2.1).

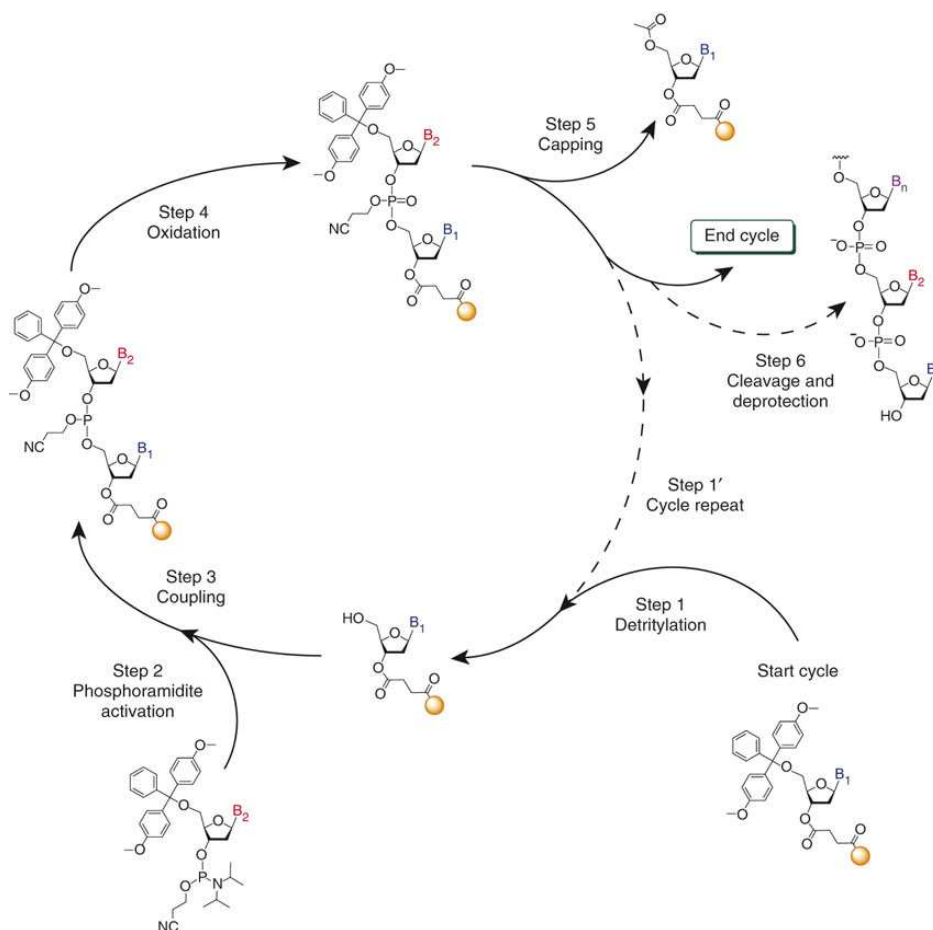


Figure 2.1. Scheme showing the steps in the solid phase synthesis of an oligonucleotide sequence<sup>5</sup>.

After the desired amount of bases is added to the sequence, one can finish the synthetic cycle and cleave the oligonucleotide from the CPG (step 6) or add a particular modifier to the surface bound chain, by following the same steps used for the coupling of a phosphoramidite. There are many different modifiers that can be used for a number of different purposes, such as labeling, anchoring or introducing new reactive groups<sup>6</sup>.

In our specific case, the modifier used was a C<sub>10</sub>-carboxy linker, 5'-Carboxy-Modifier-CE Phosphoramidite (figure 2.2), which was used to allow the synthesis of the polymer-modified oligonucleotides. The use of this linker allows the coupling of

any given compound to the oligonucleotides through formation of an amide bond, for instance, which was the chemical pathway chosen in our case and that will be discussed further on.

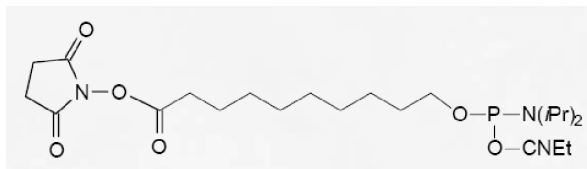


Figure 2.2. 5'-Carboxy-modifier C<sub>10</sub> coupled to the synthesized oligonucleotides in order to allow the polymer modification of the sequence.

In order to perform the cleavage of the oligonucleotides from the CPG, the steps are the following:

- 1 – Detritylation of the last added phosphoramidite, using the procedure previously described.
- 2 – Removal of the protective groups of the chain.
- 3 – Cleavage of the succinate bond between the sequence and the support, liberating the oligonucleotides, using an aqueous base.

The removal of the protective groups from the nucleotide chain will, of course, depend on the chemistry of these groups, but in general with the phosphoramidite synthesis route this can be accomplished with the use of warm ammoniac solution (40°C), which enables at the same time the cleavage of the succinate bond, combining steps 2 and 3 in a single procedure.

One must be careful, though, when using carboxy-modified oligonucleotides. The use of an ammonia solution might lead to a reaction between the carboxylic acid group and the ammonia, yielding an amide bond and, thus, preventing the use of the carboxylic functionality. To circumvent this problem, the cleavage of carboxy-terminated sequences must be performed in a sodium hydroxide methanolic solution (0.2 M NaOH in 1 : 4 H<sub>2</sub>O : Methanol)<sup>7</sup>.

Purification of the synthesized oligonucleotides is usually achieved by the use of High Performance Liquid Chromatography, HPLC, or gel electrophoresis, mainly for sequences bearing more than 50 bases. When using HPLC purification, the final detritylation of the oligonucleotides may be performed after the chromatography, in order to use the hydrophobic properties of the trityl group. The trityl residue will bind

more strongly to the column than the failed sequences, changing its elution time and yielding an oligonucleotide with higher purity.

However, some of the most troublesome impurities in the synthesis of oligonucleotides are sequences containing  $n-1$  and  $n-2$  bases, generally in a statistical distribution of all possible deletions. These faulty sequences are mainly generated by incomplete capping or unsuccessful coupling during the cycles<sup>4,8-10</sup>. These sequences also contain trityl groups, which gives them an elution time similar to that of the desired oligonucleotide. The formation of such degenerate sequences may be avoided by using a capping agent with efficiency higher than 98%, as in the case of UniCap<sup>4</sup>.

The nucleotide sequences used in this research were either synthesized using an EXPEDIT DNA Synthesizer 8909 (GMI, Inc., Ramsey, Minnesota, USA) or purchased from Operon Biotechnologies GmbH (Köln, Germany). All of the sequences used consisted of twelve deoxynucleotide units, modified at the 5'-terminus with a carboxylic group.

The oligonucleotides were acquired either still bound to CPG or HPLC purified. The expected amounts of the desired strands bound to the surface is about 75-80% of the starting material, considering a yield of 98% for each coupling step. The HPLC purified sequences were provided in the amount corresponding to the starting material synthesized.

The sequences used were the following:

- 1 – 3' GGGGGGGGGGGG [C<sub>10</sub>-carboxy] 5'
- 2 – 3' CCCCCCCCCCCC [C<sub>10</sub>-carboxy] 5'
- 3 – 3' GGGAGAGAGAGA [C<sub>10</sub>-carboxy] 5'
- 4 – 3' TCTCTCTCTCCC [C<sub>10</sub>-carboxy] 5'

Sequence 1 was chosen due to the fact that some cells may be able to recognize short poly(guanosine), polyG sequences through receptors located on their membrane<sup>11</sup>. A more statistical sequence was designed based on the same principle (sequence 3), but aiming at reaching a lower melting temperature, in order to observe the hybridization and de-hybridization of the sequence, and avoiding a repetitive sequence as well as the formation of secondary structures, such as hairpins.

Sequences 2 and 4 are fully complementary to sequences 1 and 3, respectively, also being subject to investigations.

## 2.2. Poly(butadiene)

Poly(butadiene), PB is the homopolymer obtained by the polymerization of 1,3-butadiene ( $C_4H_6$ ). The synthesis of poly(butadiene) is performed via living anionic polymerization, which generally produces polymers with a very narrow molecular weight distribution ( $M_w/M_n < 1.05$ ). This polymerization method comprises three stages, namely initiation, propagation and termination<sup>12,13</sup>.

The initiation of the polymerization is commonly done using a butyl-lithium, BuLi isomer, which dissociates in solution forming a carbanion, a negatively charged carbon chain with the charge on a carbon. The dissociation constant of the BuLi isomers increases with the branching of the butyl radical, being the *t*-BuLi much more active and dangerous to handle than *n*-BuLi.

The carbanion formed will then attack the double bonds of the butadiene, creating a new carbanion. As the polydispersity of the final polymer is directly dependant on the initiation phase, the more commonly used initiator is *sec*-BuLi, due to its fast dissociation rate.

The reaction enters then the propagation stage, in which further monomers are added to the growing polymer. It is important to notice that, being a diene, butadiene will polymerize through the reaction with either only one or both of its double bonds. In general, butadiene molecules both 1,2- and 1,4- polymerized compose the PB chains, and the ratio between them can influence the properties of the polymer, such as the glass transition temperature,  $T_g$  and the cross-linkability of the chains. It is possible, though, to control the 1,2/1,4 polymerization ratio by changing the reaction conditions of the polymerization<sup>12,13</sup>.

Once the polymerization reaches the desired conversion degree, the reaction is terminated by the addition of an electrophile, which will react with the carbanion and stop the growth of the polymeric chain, “killing” the polymerization. Commercially available poly(butadiene) is generally hydroxy terminated, but the electrophile used can also be chosen in order to fulfill specific roles or introduce particular functionalities on the polymer.

According to the synthetic choice made for the nucleo-copolymers, the poly(butadiene) chains should bear an amino termination, which was obtained by the two different methods that will be discussed in sequence.

### 2.2.1. End group modification

The first approach used to obtain amino-modified poly(butadiene) was the end group modification of the hydroxy-terminated polymer. The method used for the modification was based on the procedure utilized for the one-pot carboxy-modification of polymers<sup>14</sup>.

This technique has the advantage of being reasonably simple and leading to a high yields, which is a very important characteristic for end group modified polymers, considering that their purification is very difficult. The protocol was modified in order to accommodate the change in the resulting functionality.

The reaction of addition of the amino group to the polymer is performed in two steps (figure 2.3):

1 – The hydroxyl terminus is transformed into an alcoholate through deprotonation with potassium *tert*-butoxide, KOTBu (Sigma-Aldrich).

2 – After activation, a halide bearing the desired functional group is introduced in the reaction mixture. The polymer reacts with it through a S<sub>N</sub>2 mechanism, eliminating a halide salt and adding the desired terminal functionality to the polymer<sup>15</sup>.

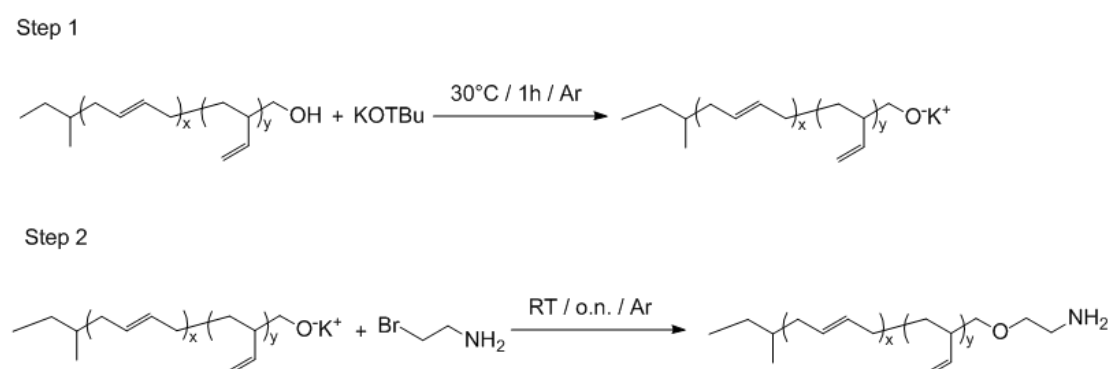


Figure 2.3. Scheme for the synthetic end group modification of poly(butadiene).

The hydroxylated PB, with a molecular weight,  $M_w = 2000 \text{ g.mol}^{-1}$ , was purchased from PolySciences, Inc. (USA). The alkylamine used to introduce the amino function in the poly(butadiene) was 2-bromoethanamine (Sigma-Aldrich).

To perform the first step of the reaction, the polymer (1 eq) was solubilized in toluene (Sigma-Aldrich). KOtBu (1.5 eq) was dissolved in *tert*-butyl alcohol and mixed in the polymer solution. The system is put under inert atmosphere ( $\text{N}_2$ ) under stirring for 1h. Activation takes place at room temperature.

The second step occurs by adding 2-bromoethanamine (5 eq) to the reaction mixture, still under inert atmosphere, under stirring. The mixture is heated up until reflux and then the heating is turned off, in order to slowly let it reach room temperature, and left over night. The haloalkylamine is not soluble in organic solvents due to the presence of the hydrobromide molecule, but under heating the complex breaks and the 2-bromoethylamine solubilizes, leaving the insoluble HBr at the bottom of the reactor. The happening of the reaction is indicated by the precipitation of salt, which increases the amount of solid material in the system.

Purification of the reaction mixture was performed by extraction with water, to remove the salt and the excess of 2-bromoethylamine from the mixture. After extraction, the organic phase was removed by rotoevaporation in order to obtain the modified polymer.

It is important to observe that, due to the molecular weight similarity between the modified PB and its precursor, the available purification techniques are not capable of separating the two materials, which is why a high reaction yield is desirable.

In order to confirm the obtention of the material in the desired yield and determine whether the integrity of the material was compromised by the reaction conditions, characterization of the polymer was performed by NMR.

NMR spectra shows that, structurally, the material is preserved, as the shifts referring to the unreacted PB and the modified PB did not suffer any alterations (figure 2.4A and 2.4B).

One can also observe the presence of solvent peaks, referring to some of the solvent used in the purification and cleaning of both the material and the vials, namely, chloroform, water acetone and tetrahydrofuran (figure 2.4B).

Unfortunately, due to the presence of these solvent peaks, direct evaluation of the yield of the reaction is hindered, as the most significant shift, related to the

addition of the haloalkylamine to the hydroxyl group at the end of the polymer chain ( $\delta(\text{O-CH}_2) = 3.76 \text{ ppm, m}$ ), is hidden. Nevertheless, it is straightforward to observe that not all the hydroxyl groups were converted, as it is still visible in the spectrum of the reacted polybutadiene ( $\delta(\text{O-H}) = 3.65 \text{ ppm, s}$ ).

The yield can be determined by comparison of the integrals of the hydroxyl shift with the PB peaks in the low field region. Using this method, the yield of the reaction can be determined as approximately 35%, which is very low, mainly considering the concerns already expressed for end group modifications. One can assume that the driving force for the substitution reaction is not high enough, since the molecule loses electrophilicity due to the presence of the amino group. This problem could be overcome by protecting the amino group before the coupling reaction.

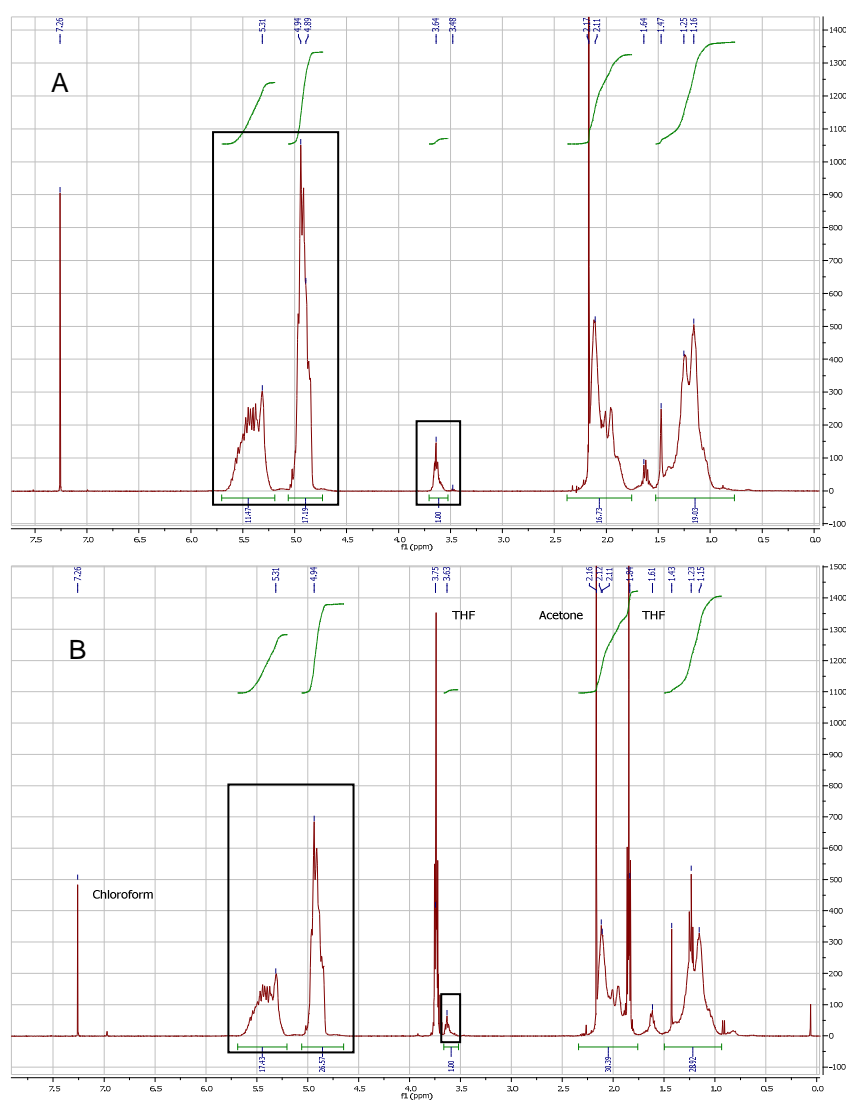


Figure 2.4. NMR spectra of A - PB-OH and B - Amino-modified PB. The highlighted areas were used to calculate the yield of the reaction.



Before any further experiments were performed in order to increase the yield of this reaction, an alternative to this method was obtained via a collaboration set with Prof. Dr. Axel Müller, in Bayreuth, Germany. His group developed a synthetic method to obtain amino-functionalized poly(butadiene) from an one-pot synthesis of PB with a high degree of control and polydispersity<sup>16</sup>.

### 2.2.2. Primary amino end-functionalized one-pot synthesis

Nosov et al.<sup>16</sup> described a method to synthesize polymers with primary amino groups by using nitrile derivatives to end-cap living anionic chain ends (termination step in anionic polymerization), followed by reduction in a one-pot process.

The synthesis of poly(butadiene) was carried out in toluene, in order to ensure high 1,4 degree of polymerization, and under pure nitrogen atmosphere. The initiator used was *sec*-BuLi and the polymerization was followed by drop of the internal pressure of the reactor.

The amino function was inserted by the use of pivalonitrile to terminate the chain growth of the living butadienyllithium. This compound was chosen due to the inexistence of protons on the  $\alpha$ -position to the nitrile group, avoiding the possibility of side reactions<sup>15</sup>, and to its relative easiness of characterization, as the *t*-butyl group can be easily identified by several analytical methods.

Following the reaction with pivalonitrile, the end-capped chains are submitted to an *in situ* reduction step with sodium borohydride ( $\text{NaBH}_4$ ). The reactions involved in the polymerization and functionalization of butadiene are shown in figure 2.5.

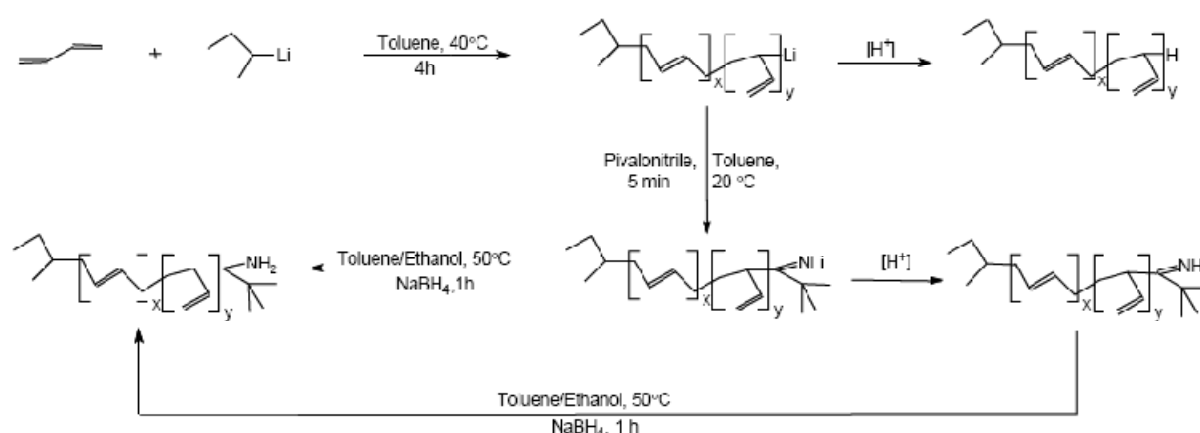


Figure 2.5. Pathway for the one-pot synthesis of amino-terminated poly(butadiene)<sup>6</sup>.

This method yielded quantitative amounts of amino-terminated 1,4-PB, with a narrow molecular weight distribution. Purification of the polymer was performed via SEC, using THF as eluent, and monitored by online refractive index detection. Characterization was performed by Matrix Assisted Laser Desorption/Ionization - Time of Flight, MALDI-ToF mass spectrometry and Nuclear Magnetic Resonance, NMR analysis.

Prof. Müller and his group were kind enough to provide us three different samples of amino-modified poly(butadiene), namely, PB<sub>2000</sub>-NH<sub>2</sub>, PB<sub>5000</sub>-NH<sub>2</sub> and PB<sub>10000</sub>-NH<sub>2</sub>, which were used for the synthesis of the polymer-modified oligonucleotides. These polymers were provided with MALDI-ToF analytic results, which were confirmed by gel permeation chromatography, GPC (table 2.1).

Polymer	MALDI-ToF		GPC	
	M <sub>w</sub> (g.mol <sup>-1</sup> )	PDI	M <sub>w</sub> (g.mol <sup>-1</sup> )	PDI
PB <sub>2000</sub> -NH <sub>2</sub>	3'450	1.02	3'554	1.10
PB <sub>5000</sub> -NH <sub>2</sub>	6'750	1.05	7'718	1.09
PB <sub>10000</sub> -NH <sub>2</sub>	26'600	1.01	29'158	1.20

Table 2.1. Molecular weight and polydispersity index, PDI of the PBs provided by Prof. Axel Müller's group.

Despite the small differences in the results shown for each of the polymers, the molecular weights of the PBs are quite consistent and within the polydispersity range. The molecular weight values used in all the calculations involving these polymers from this point on were performed using the values obtained by GPC analysis.

In order to avoid possible degradation of the poly(butadiene)s, by cross-linking, for example, the polymers were stored in sealed vials under argon atmosphere at room temperature, away from light and any heat source.

These PBs were then used to perform the synthesis of the polymer-modified oligonucleotides.

## 2.3. Polymer-modified Oligonucleotides

The synthesis of the nucleotide-based amphiphilic diblock copolymers, nucleo-copolymers, was performed by coupling the modified oligonucleotides to the amino-terminated poly(butadiene) via an amide linkage.

Amide bonding presents very interesting characteristics, such as general high yields and mild reaction conditions, besides easiness of handling. These are attractive traits for the synthesis, mainly if one considers the stability of oligonucleotides. Furthermore, the peptide bond is kinetically stable to hydrolysis, which only occurs in boiling alkali or in strong acidic conditions<sup>15,17</sup>.

The formation of the amide bond between carboxylic acids and amines is a kinetically slow reaction due to the low  $pK_a$  of carboxylic acids. In order to increase their electrophilicity, the carboxylic groups must be activated, what is achieved by the utilization of an activator.

The most common activators used in the formation of peptide bonds are carbodiimides. These compounds bind to the carboxylate groups, making them more available for the reaction with the amines, acting as leaving groups and carrying the water molecules eliminated in the course of the reaction. Dicyclohexylcarbodiimide, DCC and diisopropylcarbodiimide, DIC are the generally used carbodiimides, but the latter presents some advantages when compared to the former, mainly due to the high solubility of the DIC-derivatives formed during the reaction, much easier to separate than the ones from DCC<sup>18</sup>.

The nucleo-copolymers were obtained by two different reaction pathways, although both using amide linkage between the oligonucleotides and the polymers. These two methodologies were developed in order to match specific needs from a synthetic point of view and will be discussed in further detail.

### 2.3.1. Solid Phase Chemistry<sup>19,20</sup>

The first methodology utilized in the synthesis of nucleo-copolymers was the chemistry on solid phase. Having the oligonucleotides bound to the CPG during the synthesis and addition of the carboxylic group to its 5'-terminus, we have chosen to perform the coupling of the amino-modified PB before cleaving the oligonucleotides

from the support. This method allowed the synthesis of the nucleo-copolymer bound to the CPG<sup>19</sup>.

This technique presents the advantage of avoiding long and tedious purification steps to obtain the final product: once the copolymer is bound to the support, all other species present in the reaction mixture can be easily washed away, remaining only the desired compound.

This reaction was performed using a TWIST™ column (Glen Research, USA), in which the CPG bearing the oligonucleotides was placed. Having the carboxy modified oligonucleotides as limiting reagent (1 eq), a solution containing 10 eq of poly(butadiene) in 1.0 mL of dichloromethane, DCM was prepared and added to the reactor. The activation agent DIC was also added (1.5 eq) and the mixture was agitated over night at room temperature. The reaction was performed for a long time period (14-16h) in order to allow maximum conversion.

After the reaction was completed, the solution in the reactor, now containing unreacted PB and consumed activator in DCM, was sucked out through one of the frits of the reactor, leaving only the CPG and the nucleo-copolymer bound to it. The support was then washed 5 times with pure DCM, in order to remove any material unbound to the glass beads.

The next step was the cleavage of the nucleo-copolymer from the support, which was done with a 32% solution of ammonia. The CPG linked to the copolymer was transferred to an Eppendorff vial and 1 mL of the cleavage solution added. The cleavage was performed over night at 40°C under shaking.

Following the cleavage, the polymer modified oligonucleotides are now free in the solution and the support can be removed via filtration. The nucleo-copolymer solution was then lyophilized in order to be prepared for purification.

Although solid phase chemistry prevents multi-step and complex purification, it is a fact that an amide bond is never formed with a 100% yield. Hence, some of the nucleotide sequences on the resin did not couple to the PB and, after cleavage, remained in the solution. In order to remove these undesired species from the product, size exclusion chromatography, SEC in aqueous phase was employed.

SEC was performed using glass columns (BioRad, USA) and Sepharose 4B (Fluka) as chromatographic agent while the eluting solution was phosphate buffer saline, PBS. The chromatography was followed through real-time UV detection.

The chromatograms obtained in SEC (figure 2.6) showed two distinct fractions: the first one with shorter elution time, which was supposed to be the nucleo-copolymer, probably already self-assembled, and a second one, with a much longer elution time, which was assumed to be the unreacted oligonucleotide. It was interesting to notice that the second peak was always more intense than the first one, which is due to the fact that the scattering of the light by the self-assembled structures tends to reduce the intensity of the UV signal in the first fraction.

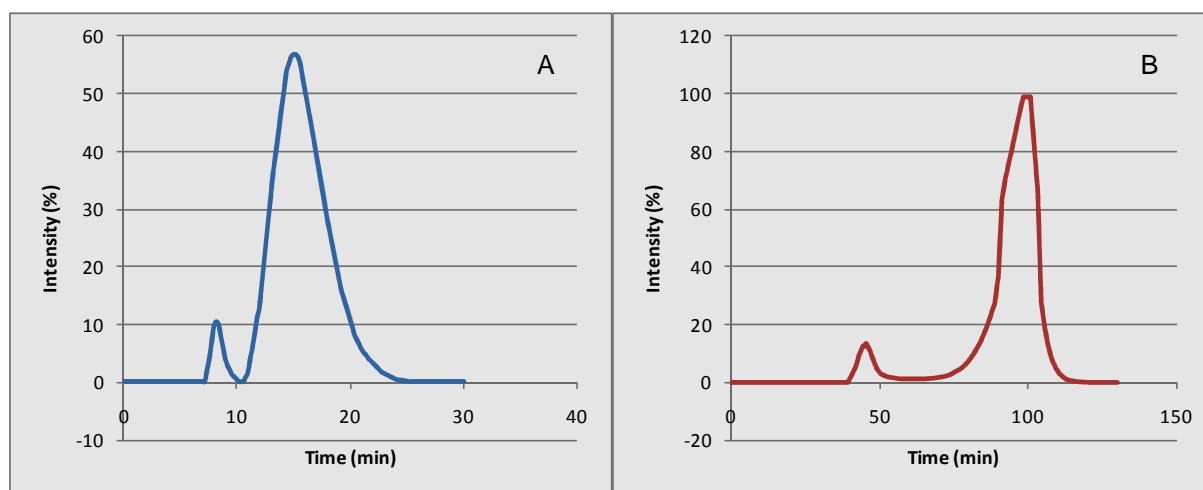


Figure 2.6. SEC chromatograms for  $C_{12}$ -PB<sub>2000</sub> (A) and  $G_{12}$ -PB<sub>2000</sub> (B) in PBS buffer.

In order to characterize the material, it was necessary to, firstly, reduce the volume of the fraction and, secondly, remove the salt present in the buffer to obtain the pure nucleo-copolymer.

Ultrafiltration was performed using Centricon filters (cutoff 3'000 Da, Millipore). The solution was added to the filters and then centrifuged at 4'000 rpm for 30 minutes. After the process, the retentate was collected and the filtrate disposed. Unfortunately, the use of Centricon filters proved not to be a suitable choice for this process, since precipitation of material onto the membrane was observed, indicating that the material was binding to it.

Lyophilization, or freeze-drying, was, then, chosen as an alternative to ultrafiltration in order to concentrate the material. It was performed by freezing the solution in 14 mL lyophilization Falcon<sup>®</sup> tubes (BD Biosciences, USA), which was further submitted to low pressures at room temperature, RT. According to the colligative properties of water, it sublimates in these conditions, leaving only the

solute behind. Lyophilization was performed beforehand due to the large volume of solution obtained by SEC.

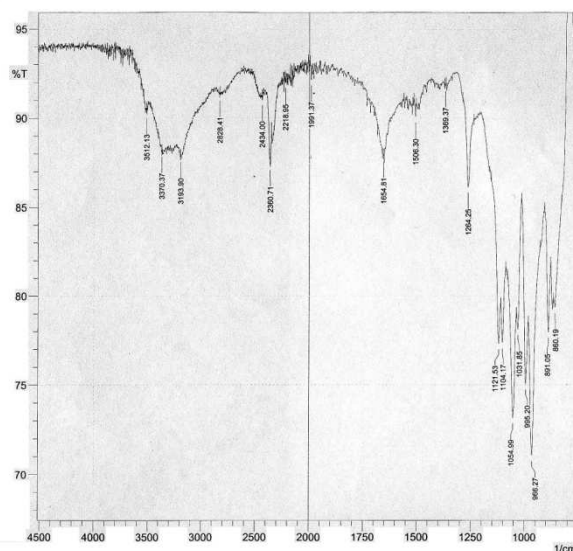
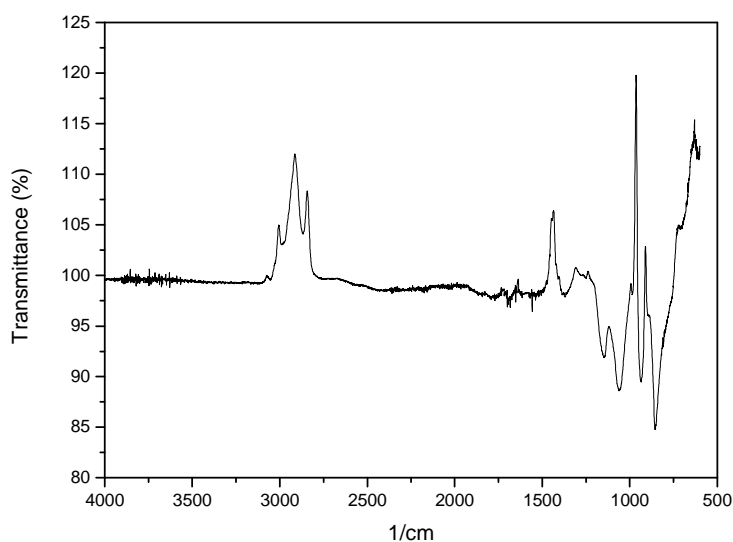
After being lyophilized, the material obtained, composed of nucleo-copolymer and salts, was redissolved in a small volume of bi-distilled water and then dialyzed. Dialysis was carried out using a Slide-o-lyzer (3 mL volume, cutoff 3'500 Da, Pierce Biotechnology, Thermo Fisher Scientific) against bi-distilled water for 24h. The dialyzed solution was then transferred to a lyophilization Falcon<sup>®</sup> tube and once again lyophilized.

The dry lyophilized material was the nucleo-copolymer, of which the chemical and physical chemical characterization was performed. The yield of the reaction, regretfully, could not be determined with precision. This is due to the simple reason that the actual load of oligonucleotides on the CPG was not known accurately, as it's impossible to predict how many of the nucleotide chains did actually grow fully. Nevertheless, based on the theoretical oligonucleotides load, we could calculate that the yield of the reaction was of approximately 60-70%, in average.

The chemical characterization of the nucleo-copolymers was performed using several techniques, namely, Fourier Transform Infrared, FT-IR spectroscopy and Electrospray Ionization Mass Spectrometry, ESI-MS. Other techniques such as MALDI-ToF mass spectrometry and NMR were also attempted, but with much less successful results.

FT-IR measurements were performed in two different ways. Firstly, air was used as the background for the analysis, which enabled the assignment of the peaks<sup>15</sup> relates to the PB ( $1620-1680\text{ cm}^{-1}$  ( $\nu_{\text{C}=\text{C}}$ );  $2853-2962\text{ cm}^{-1}$  ( $\nu_{\text{C}-\text{H}}$ )) as well as those that belong to the oligonucleotide sequences ( $3500-3700\text{ cm}^{-1}$  ( $\nu_{\text{O}-\text{H}}$ );  $3300-3500\text{ cm}^{-1}$  ( $\nu_{\text{N}-\text{H}}$ );  $1250-1335\text{ cm}^{-1}$  ( $\nu_{\text{C}-\text{N}-\text{C},\text{ar}}$ );  $1104-1121\text{ cm}^{-1}$  ( $\nu_{\text{P}=\text{O}}$ );  $1000-1300\text{ cm}^{-1}$  ( $\nu_{\text{C}-\text{O}-\text{C},\text{cycl}}$ )). But more importantly, the shifts corresponding to the peptide bond ( $3100-3500\text{ cm}^{-1}$  ( $\nu_{\text{N}-\text{H}}$ );  $1640-1690\text{ cm}^{-1}$  ( $\nu_{\text{C}=\text{O}}$ )) were also observed (Figure 2.7).

A second methodology applied for the FT-IR measurements was the use of PB as the background. This method permitted the observance of only the oligonucleotide-related peaks, as well as the negative shifts corresponding to the introduction of the alkyl group of the C<sub>10</sub>-linker by formation of the amide bond between the blocks of the nucleo-copolymer ( $\nu_{\text{C}-\text{H}} = 2853-2962\text{ cm}^{-1}$ ) (figure 2.8).

Figure 2.7. FT-IR measurement of  $C_{12}$ -*b*- $PB_{2000}$ .Figure 2.8. FT-IR of  $G_{12}$ - $PB_{2000}$  on  $PB_{2000}$  background.

Both methodologies showed that the formation of the amide bond between the oligonucleotide and the PB occurred, which indicates the synthesis was successful. In order to prove beyond doubt that synthetic approach for the synthesis of nucleo-copolymers was valid, ESI-MS was performed.

ESI-MS was performed on a sample in Tris-EDTA, TE buffer, which is a widely used solution for the storage of oligonucleotides<sup>21</sup>. Through the spectrogram obtained (figure 2.9) the shifts related to the nucleo-copolymer were identified and, once again, the success of the solid phase synthesis was proven.

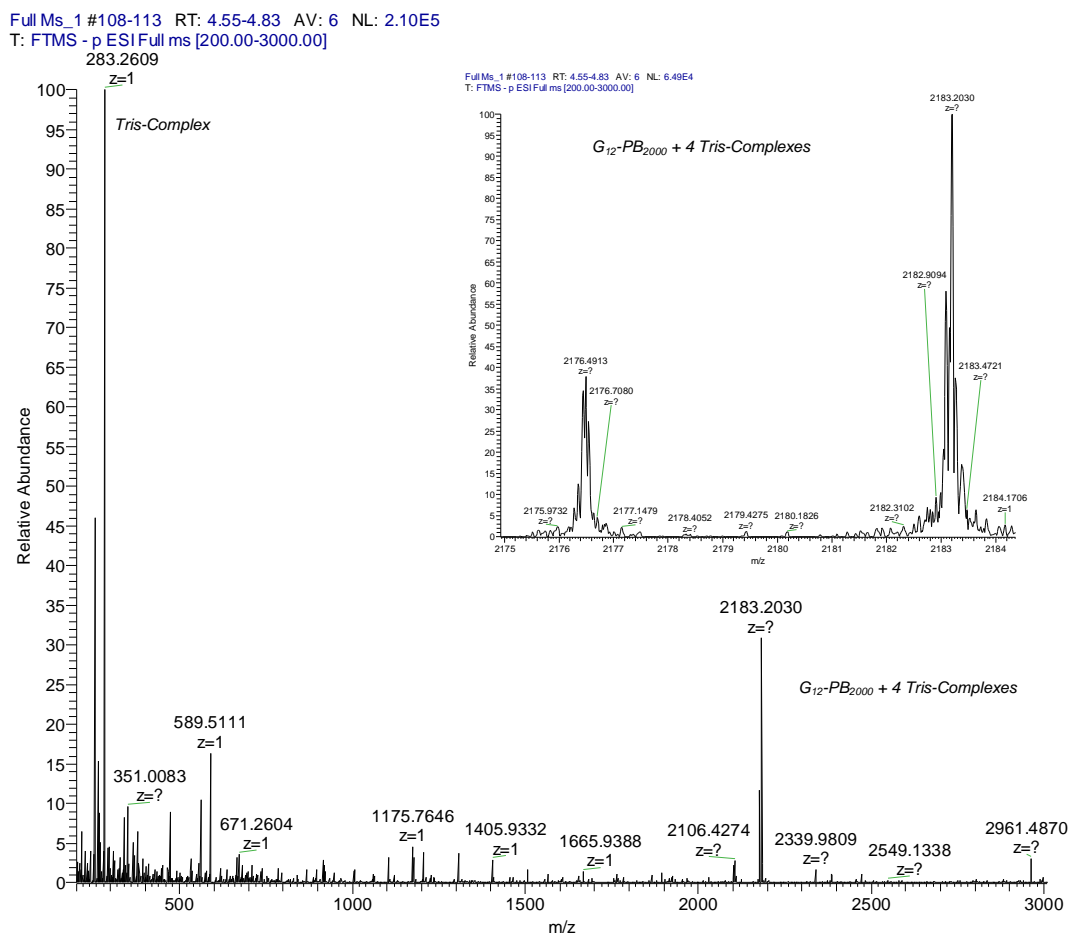


Figure 2.9. ESI-MS spectra for  $G_{12}$ -PB<sub>2000</sub>, measured from a TE buffer solution.

The relevant peaks, as well as the composition of the material to which they correspond, are shown in table 2.2.

M <sub>w</sub> (g.mol <sup>-1</sup> )							
G <sub>12</sub>	Linker	PB <sub>2000</sub>	G <sub>12</sub> <sup>-</sup> -PB <sub>2000</sub>	Tris	Tris <sub>2</sub>	Tris <sub>2</sub> -HCl (A)	Tris <sub>2</sub> -NaCl (B)
3888	154	3554	7596	121	242	277,5	300,5
G <sub>12</sub>		G <sub>12</sub> -Tris	G <sub>12</sub> -PB <sub>2000</sub>	G <sub>12</sub> -PB <sub>2000</sub> + A	G <sub>12</sub> -PB <sub>2000</sub> + 2A	G <sub>12</sub> -PB <sub>2000</sub> + 3A	G <sub>12</sub> -PB <sub>2000</sub> + 4A
z	m/z						
1	3888,0	4009,0	7596,0	7873,5	8151,0	8428,5	8706,0
2	1944,0	2004,5	3798,0	3936,8	4075,5	4214,3	4353,0
3	1296,0	1336,3	2532,0	2624,5	2717,0	2809,5	2902,0
4	972,0	1002,3	1899,0	1968,4	2037,8	2107,1	2176,5
5	777,6	801,8	1519,2	1574,7	1630,2	1685,7	1741,2
6	648,0	668,2	1266,0	1312,3	1358,5	1404,8	1451,0
7	555,4	572,7	1085,1	1124,8	1164,4	1204,1	1243,7
8	486,0	501,1	949,5	984,2	1018,9	1053,6	1088,3
9	432,0	445,4	844,0	874,8	905,7	936,5	967,3
10	388,8	400,9	759,6	787,4	815,1	842,9	870,6
11	353,5	364,5	690,5	715,8	741,0	766,2	791,5
12	324,0	334,1	633,0	656,1	679,3	702,4	725,5

Table 2.2. Relation between molecular weight and ionization (m/z) for  $G_{12}$ -b-PB<sub>2000</sub> taking into account the formation of different complexes formed during the analysis.



We cannot explain whether there is an actual reason why we observed an ionization number  $z = 4$  in the sample, but one can observe that with this number the fitting between the calculated and the measured values leads to an exact match between them. Likewise, it is also difficult to conclude on what kind of complex is formed by the tris salt during the analysis. However, analysis of the data obtained led us to believe that tris forms a complex with HCl in the form of  $\text{tris}_2\text{-HCl}$ , as it's the value that closer relates to the experimental results.

As previously mentioned, MALDI-ToF analysis was also attempted. Unfortunately, the spectrograms obtained did not allow any conclusions. This could be easily explained by the fact that the two blocks that compose the nucleo-copolymer are, already separately, quite difficult to measure through this technique.

Oligonucleotides, though crystallizable, are quite sensitive to the ionization process, requiring an appropriate matrix, such as 3,4-diaminobenzophenone (DAPB), and a lower laser intensity in order to be analyzed by MALDI-ToF<sup>22</sup>. Unfortunately, the characteristics of the PB are exactly the opposite, since it is a non-crystalline polymer and, therefore, very hard to observe at low laser intensities.

These antagonistic properties made it very difficult to analyze the nucleo-copolymer, even though the DNA suitable matrix and a general one (2,5-dihydroxybenzoic acid) were used.

After synthesis, the nucleo-copolymer could not be fully dissolved in any solvent, either presenting some degree of aggregation, in more polar solvents, or not being soluble at all, in the case of apolar ones. Water was the solvent in which the best solubility was achieved, but always upon spontaneous self-assembly, which will be discussed further ahead (Chapter 3: Self-Assembly).

This highly amphiphilic behavior of the nucleo-copolymer also prevents performing NMR analysis, given that the size of the structures present in the solution led to very small diffusion times (in the order of  $10^{-12}$ - $10^{-13}$  m<sup>2</sup>/s, measured by dynamic light scattering), which are beyond the detection limit of solution NMR. As no theta solvent for the nucleo-copolymers was found, the NMR spectra obtained for all the analyses performed did not yield any relevant information about the composition or structure of the polymer-modified oligonucleotides.

### 2.3.2. Heterogeneous Biphasic Chemistry<sup>20</sup>

Despite the fact that solid phase synthesis proved to be a very simple and straightforward method for the production of nucleo-copolymers, one limitation to this chemical route remained: the possibility of steric impediments for the reaction to occur on the solid support. If one uses very long nucleotide sequences and/or polymeric chains to synthesize the nucleo-copolymer, the yield of the reaction drops dramatically due to the hindering of diffusion through the pores of the CPG<sup>1</sup>.

In order to overcome this issue, a new synthetic methodology had to be developed, in which diffusional limitations would not be a problem for the synthesis. Thus, the Heterogeneous Biphasic Chemistry, BHC route was designed (figure 2.10).

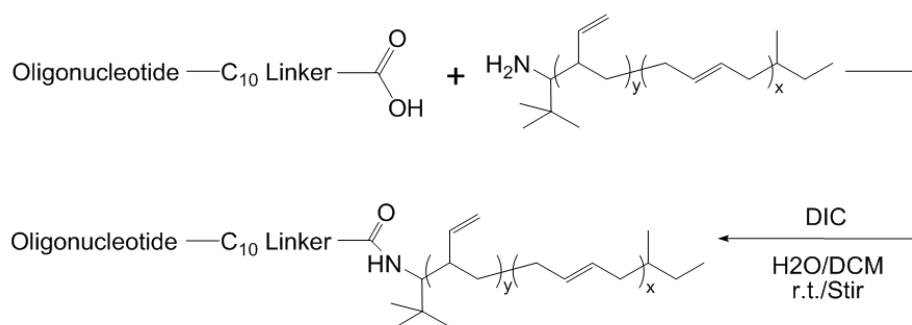


Figure 2.10. Scheme of the Biphasic Heterogeneous Chemistry, BHC synthetic route.

The BHC takes advantage of the same characteristics and properties of the starting materials utilized in solid phase synthesis, but instead of having the reaction taking place on surface of the solid support, it now occurs at the interface between the solvents in which the starting materials are solubilized.

The carboxy-modified oligonucleotides were cleaved from the CPG and dissolved in pure, bi-distilled water. Although fully soluble, the carboxylic modified terminus still presents an intrinsic hydrophobicity due to the carbonic chain used to introduce this modification. Given the possibility, this lipophilic tail would solubilize in an apolar environment. Once a biphasic system, composed by water and an organic solvent, such as dichloromethane, DCM, is prepared and mixed, one can assume that the hydrophobic modification on the nucleotide sequences is drawn to the interface, where the carboxylic group is exposed to the apolar phase.

In its turn, the organic solvent would contain the hydrophobic amino-terminated block and the peptide bond formation would occur at the interface.

Provided that the system is put under strong stirring, i.e. increasing the reactive area between the phases, the resulting nucleo-copolymer should be obtained in a quantitative yield. Another advantage of this method is that we are no longer limited to small scale syntheses, as with the solid phase approach.

The final element for the methodology to work would be the activator, which should be stable under the reaction conditions. There are concerns regarding carbodiimides in aqueous solutions, as they should spontaneously react in contact with water and yield their urea derivative<sup>18</sup>.

In order to observe the stability of the activator to the reaction conditions, a blank system, without oligonucleotide or poly(butadiene), was prepared. DIC was solubilized in DCM, put together with pure, bi-distilled water and strongly stirred overnight. After completion of the reaction time, the two fractions were extracted and concentrated. The material recovered was collected and thereafter NMR (figure 2.11) and FT-IR (figure 2.12) analyses were performed.

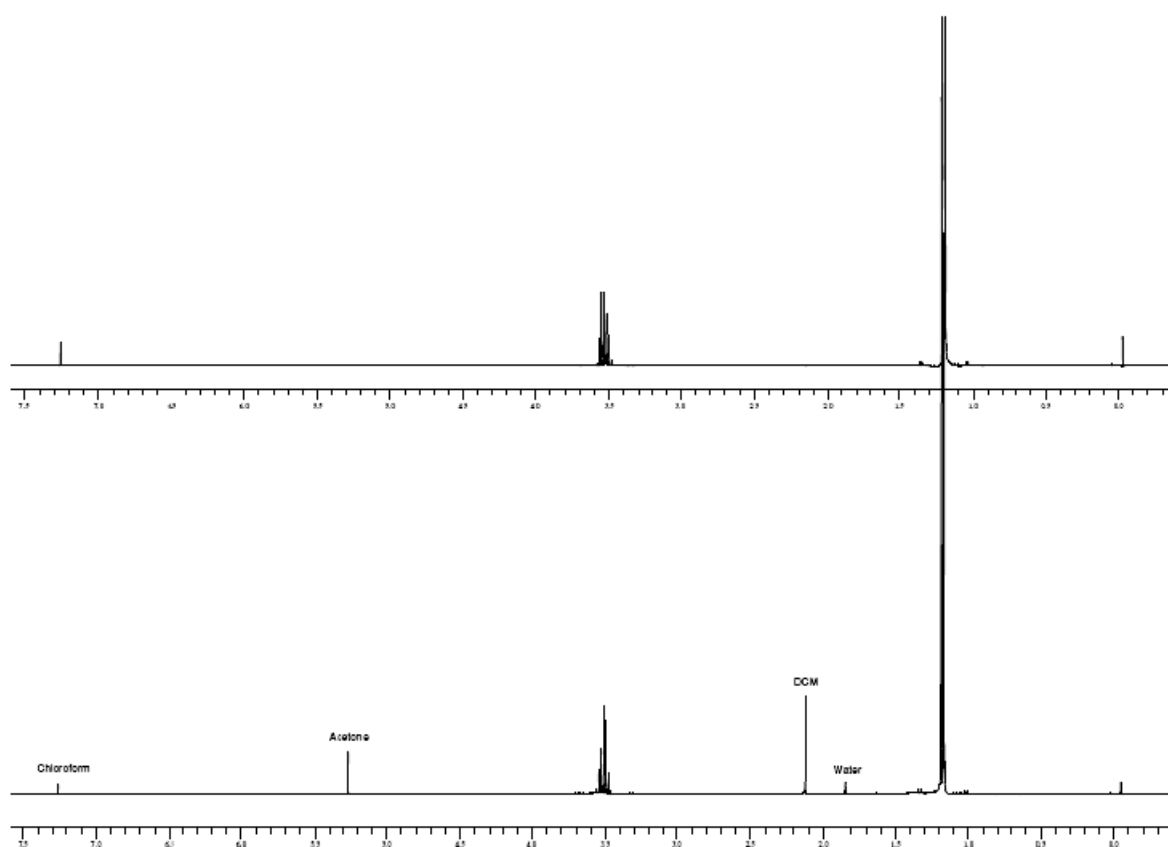


Figure 2.11. <sup>1</sup>H-NMR spectra from DIC before (top) and after (bottom) being submitted the BHC reaction conditions.

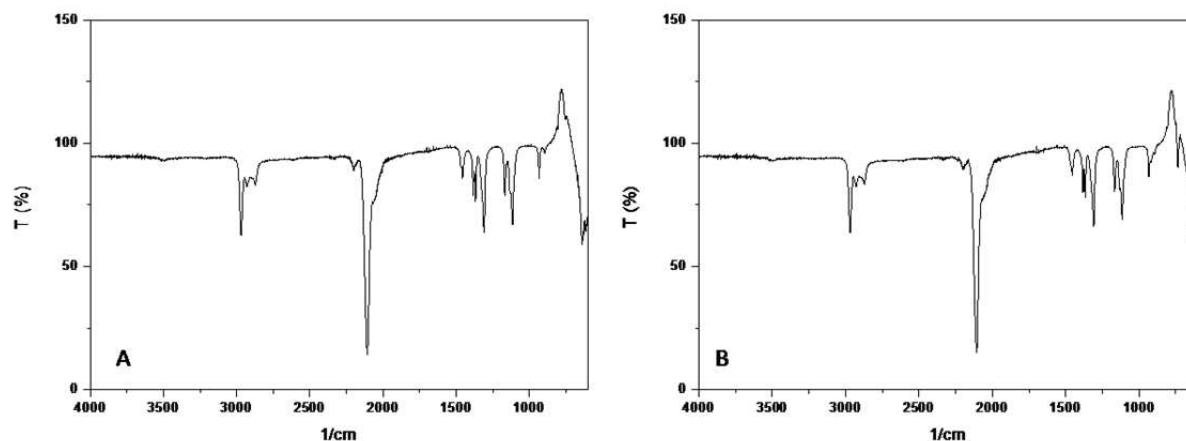


Figure 2.12. FT-IR spectra of DIC before being submitted to the BHC reaction conditions (A) and after (B).

The results of the analyses showed that DIC did not suffer any structural change due to the contact with water, being still capable of initiating the amide bond formation. This was probably a result of the fact that previous to being put in contact with water DIC was dissolved in the organic solvent, which prevented the decomposition of the activator.

The synthesis was performed using a 1  $\mu\text{M}$  aqueous oligonucleotide solution (1 eq) and a 0.5  $\mu\text{M}$  PB solution (10 eq) in DCM, with 1.5 eq of the activator, DIC. The two solutions were put together in a vial and stirred strongly for 24 h, in order to allow maximum conversion of the reactants.

When synthesis time was complete, the stirring was stopped and the two phases were allowed to segregate for a couple of hours, after which the fractions were separated. Considering that the product of the BHC synthesis is an amphiphilic molecule produced at an interface, it is not clear where the material would be solubilized after the reaction, once it could self-assemble in either of the phases. Both fractions were then concentrated (the aqueous phase through lyophilization and the organic one through rotoevaporation) and prepared for SEC.

Chromatography of the aqueous phase was performed in PBS buffer using Sepharose 4B as the gel separation media, as previously described. To perform the size exclusion chromatography on the organic phase, a new system was prepared specifically to be used with apolar solvents. The gel separation media utilized was Biobeads S-X1 (Biorad) in glass columns (Biorad) and using DCM or chloroform as the eluent. The chromatography was monitored by online UV detection (figure 2.13).

Each of the samples, from the organic and aqueous phase, yielded two fractions of material in the size exclusion chromatogram. Depending on the length of

the hydrophobic block coupled to the oligonucleotide, the amount of it in each phase changes, hence the importance of purifying both of them.

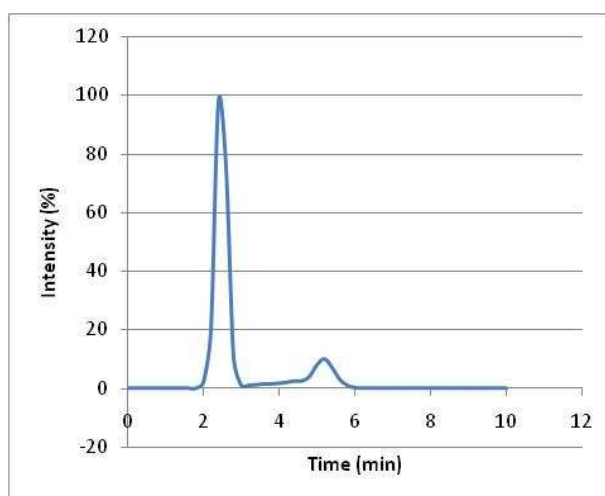


Figure 2.13. Organic phase SEC chromatogram of the copolymer  $G_{12}$ - $b$ - $PB_{5000}$ .

After SEC, the fractions containing the nucleo-copolymer were concentrated through dialysis and lyophilization (aqueous phase) and rotoevaporation (organic phase) and prepared for characterization. The techniques employed were GPC, NMR and FT-IR.

The copolymer synthesized, while bearing a longer PB chain, was now soluble in organic solvents, such as chloroform. Therefore, characterization through GPC could be attempted. Unfortunately, the chromatogram obtained did not reveal any shift that could be correlated to the nucleo-copolymer, but rather a peak that was clearly PB.

This result led to two conclusions: the first that the filtration step in the sample preparation for GPC probably retained the nucleo-copolymer, since regardless of being soluble in chloroform, it still had some degree of self-assembly due to its amphiphilicity.

The second conclusion was that the purification of the nucleo-copolymer by SEC was incomplete, although the fraction separation was clear in the chromatogram. This could be also related to the amphiphilicity of the material, which could have entrapped some of the unreacted poly(butadiene) in the self-assembled structures. New SECs were performed, using a longer resin bed, in order to better

purify the nucleo-copolymer, but GPC was abandoned as a characterization technique.

FT-IR analyses were performed using poly(butadiene) as background for the analysis of the PB<sub>5000</sub>-based copolymers (figure 2.14).

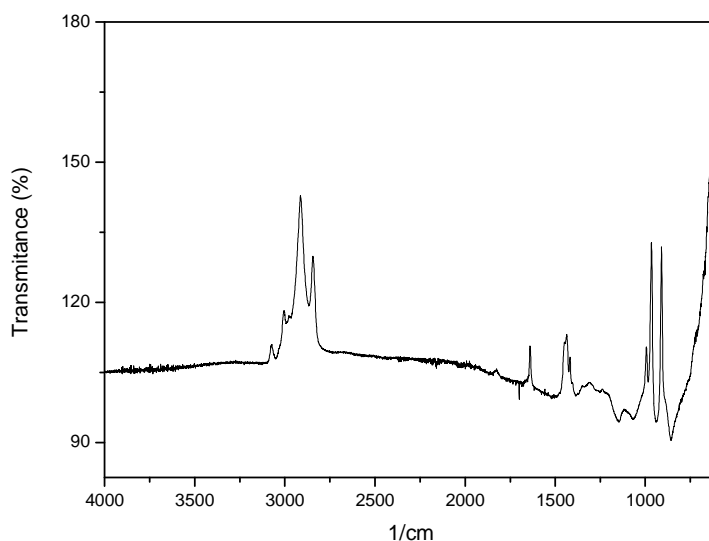


Figure 2.14. FT-IR analysis of G<sub>12</sub>-*b*-PB<sub>5000</sub> using PB<sub>5000</sub> as background.

The spectra revealed that the coupling between the oligonucleotide and the polymer was successful, given the negative shift related to the introduction of the alkyl group of the C<sub>10</sub>-linker ( $\nu_{C-H} = 2853\text{--}2962\text{ cm}^{-1}$ ) and the presence of the nucleotide shifts, in the range of 750 to 1500  $\text{cm}^{-1}$ .

Due to some changes observed in the physical properties of the copolymers, color modification, for instance, new FT-IR measurements were performed and the intensity of the peaks related to the oligonucleotide was rather weak. This raised some suspicion about the stability of the nucleo-copolymer in organic media, as it was stored during the time necessary for purification and characterization in CHCl<sub>3</sub>.

Nevertheless, FT-IR analyses show that BHC is an efficient method in the synthesis of polymer-modified oligonucleotides.

NMR measurements were once again performed, in the hope that the solubility of the oligonucleotide-based block copolymers in organic solvents would allow the obtention of suitable spectra to characterize the copolymer. Unfortunately, as previously discussed, the self-assembling phenomenon also takes place in organic solvents, such as CHCl<sub>3</sub>, and none was found to present theta properties.

Therefore, the same limitations inherent to the NMR analysis of PB<sub>2000</sub>-based copolymers are also observed for those bearing PB<sub>5000</sub> and PB<sub>10000</sub> chains.

## 2.4. References

1. Blackburn, G.M. DNA and RNA structure. In *Nucleic Acids in Chemistry and Biology*, 2<sup>nd</sup> Edition; Blackburn, G.M., Gait, M.J., Eds.; Oxford University Press: New York, NY, USA, 1996.
2. Beaucage, S.L., Oligodeoxyribonucleotide synthesis: phosphoramidite approach. In *Protocols for Oligonucleotides and Analogs, synthesis and properties*; Agrawal, S., Ed.; Humana Press Inc.: Totowa, NJ, 1993; Volume 20.
3. Glen Research website: <http://www.glenresearch.com//Catalog/supports.html>, visited on 28/01/2009.
4. Glen Research, Glen Report, Volume 17, Number 1, September, 2004.
5. Greco, N.J.; Tor, Y. Synthesis and site-specific incorporation of a simple fluorescent pyrimidine, *Nat. Protoc.* **2**, **2007**, 305-316.
6. Glen Research website: <http://www.glenresearch.com//Catalog/modifiers.html>, visited on 30/01/2009.
7. Glen Research, Glen Report, Volume 15, Number 1, March, 2002.
8. Tamsamani, J.; Kubert, M.; Agrawal, S. Sequence identity of the n-1 product of a synthetic oligonucleotide. *Nucleic Acids Res.* **1995**, *23*, 1841-1844.
9. Fearon, K.L.; Stults, J.T.; Bergot, B.J.; Christensen, L.M.; Raible, A.M. Investigation of the 'n-1' impurity in phosphorothioate oligodeoxynucleotides synthesized by the solid-phase  $\beta$ -cyanoethyl phosphoramidite method using stepwise sulfurization. *Nucleic Acids Res.*, **1995**, *23*, 2754-2761.
10. Chen, D.; Yan, Z.; Cole, D.L.; Srivatsa, G.S. Analysis of internal (n-1)mer deletion sequences in synthetic oligodeoxyribonucleotides by hybridization to an immobilized probe array. *Nucleic Acids Res.*, **1999**, *27*, 389-395.
11. Broz, P.; Benito, S.M.; Saw, C.; Burger, P.; Heider, H.; Pfisterer, M.; Marsch, S.; Meier, W.; Hunziker, P. Cell targeting by a generic receptor-targeted polymer nanocontainer platform. *J. Control. Release*, **2005**, *102*, 475-488.
12. Nicholson, J.W. *The Chemistry of Polymers*, 3<sup>rd</sup> Edition; RCS Publishing: Cambridge, UK, 2006.

13. Hsieh, H.L.; Quirk, R.P. *Anionic Polymerization: Principles and Practical Applications*; Marcel Dekker: New York, NY, USA, 1996.
14. Greenwald, R.B.; Gilbert, C.W.; Pendri, A.; Conover, C.D.; Xia, J.; Martinez, A. Drug Delivery Systems: Water Soluble Taxol 2'-Poly(ethylene glycol) Ester Prodrugs Design and in Vivo Effectiveness. *J. Med. Chem.*, **1996**, *39*, 424-431.
15. Solomons, T.W.G.; Fryhle, C.B. *Organic Chemistry*, 7<sup>th</sup> Edition; John Wiley and Sons, Inc.: New York, NY, USA, 2000.
16. Nosov, S.; Schmalz, H.; Müller, A. H. E. One-pot synthesis of primary amino end-functionalized polymers by reaction of living anionic polybutadienes with nitriles. *Polymer* **2006**, *47*, 4245-4250.
17. Pine, S.H. *Organic Chemistry*, 5<sup>th</sup> Edition; McGraw-Hill Book Co.: Singapore, 1987.
18. Ulrich, H. *Chemistry and Technology of Carbodiimides*; John Wiley and Sons, Inc.: New York, NY, USA, 2007.
19. Teixeira Jr., F.; Rigler, P.; Vebert-Nardin, C. Nucleo-copolymers: Oligonucleotide-based amphiphilic diblock copolymers. *Chem. Comm.* **2007**, *11*, 1130-1132.
20. Teixeira Jr., F.; Nussbaumer, M.; Syga, M.-I.; Nosov, S.; Müller, A.H.E.; Vebert-Nardin, C. Polymer-modified oligonucleotides: synthesis and characterization of biologically active self-assembled interfaces. *In preparation*.
21. Sambrook, J.; MacCallum, P. *Molecular Cloning, A Laboratory Manual*, 3<sup>rd</sup> Edition; Cold Spring Harbor Laboratory Press: New York, NY, USA, 2001.
22. Castleberry, C.M.; Chou, C.-W.; Limbach, P.A. Matrix-Assisted Laser Desorption/Ionization Time-of-Flight Mass Spectrometry of Oligonucleotides. In *Current protocols in nucleic acid chemistry*; Beaucage, S.L., Ed.; John Wiley and Sons, Inc.: New York, NY, USA, 2007.



## Chapter 3: Self-Assembly

Self-assembly is the phenomenon through which macromolecules spontaneously form structures at a higher level of organization than that achieved by the isolated molecules due to one or more intra- or intermolecular interactions (specific or not). This process is well known<sup>1,2</sup> and can be observed in many natural macromolecules with an impressively high degree of specificity.

Proteins, for instance, which are peptide sequences, spontaneously assume secondary structures identified as  $\alpha$ -helices or  $\beta$ -sheets. Depending on the peptide composition, folding into more complex structures gives the protein its functional role in the metabolism<sup>3,4</sup>. The formation of the DNA double helix is yet another example of highly specific natural self-assembly, driven by the interaction between the bases that compose each of the strands<sup>3,5</sup>.

Thermodynamically<sup>1,2</sup>, the formation of highly organized macromolecular structures implies the loss of entropy in the system, which normally is a non-spontaneous process. However, the existence of interactions between the molecules in the self-assembly, which favors the formation of these structures, provides an enthalpic contribution to the overall energy balance. Whenever such interactions occur, the entropic loss is outweighed by the gain in enthalpy, rendering the formation of more organized structures favorable.

The main interactions involved in the self-assembly phenomenon are: 1) H-bonds, 2) Van der Waals forces, 3) hydrophobic interactions and 4)  $\pi$ - $\pi$  stacking. In general, these interactions do not occur separately, but a combination of them is responsible for the morphological characteristics of the self-assembled structures<sup>2</sup>.

### 3.1. Block Copolymers

In the specific case of block copolymers, which is the one relevant to this work, the self-assembly of macromolecules is highly dependent on their composition and environmental conditions. The amphiphilicity of the molecules and the physical chemical incompatibility between its building blocks will be defining elements for the morphology of the self-assembly<sup>6-9</sup>. Composition, length, conformation and

configuration of the molecules will drive the self-assembly process of amphiphilic block copolymers into a specific morphology.

Besides the number of blocks in the copolymer, the volume fraction between them has a critical role in the self-assembly of the copolymers<sup>7</sup>. Some of the most canonic geometries of self-assembled structures from block copolymers, both in the bulk and in solution, can be observed in figure 3.1.

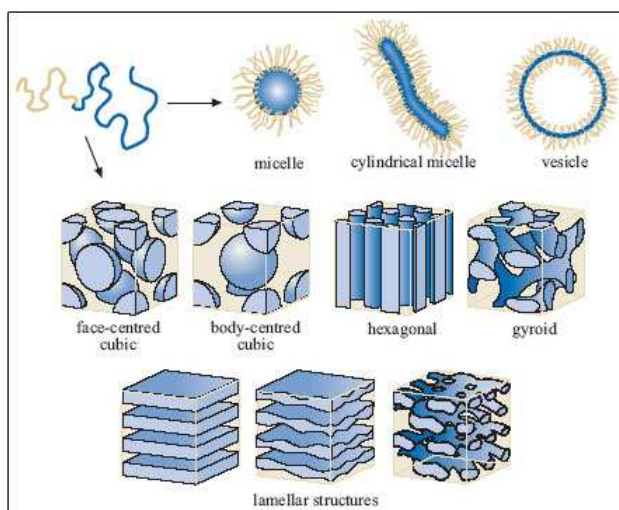


Figure 3.1. Self-assembled structures formed by block-copolymers in solution and in bulk.

In the bulk, the blocks of the copolymer undergo micro-phase segregation, yielding a solid with distinct compositions in different domains and with a well-defined geometry<sup>8,9</sup>. By adding a selective solvent to the copolymer, the geometry of the self-assembled macromolecules starts to change, as the material swells and ceases being a solid, becoming a gel. With the further increase of the solvent content, the mixture changes into a solution, in which the block copolymers are self-assembled and loosely dispersed in the solvent (figure 3.2).

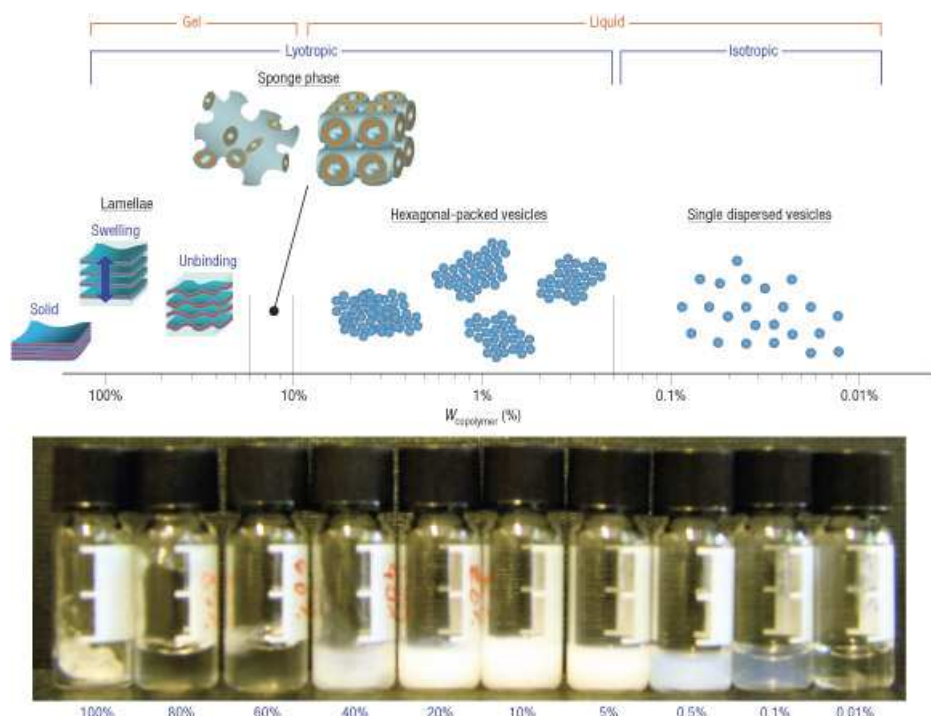


Figure 3.2. Diagram showing the modification in the geometry of a self-assembling block copolymer from lamellar bulk to vesicles as a function of the water content in the solution<sup>10</sup>.

The solvent effect on the self-assembly of block-copolymers has been also well described<sup>11</sup>. It is shown that an inversion of the polarity of the solution from polar to apolar will lead to a morphological change in the self-assembled structures of block-copolymers, going from micelles to inverse micelles, and also size modification (figure 3.3).

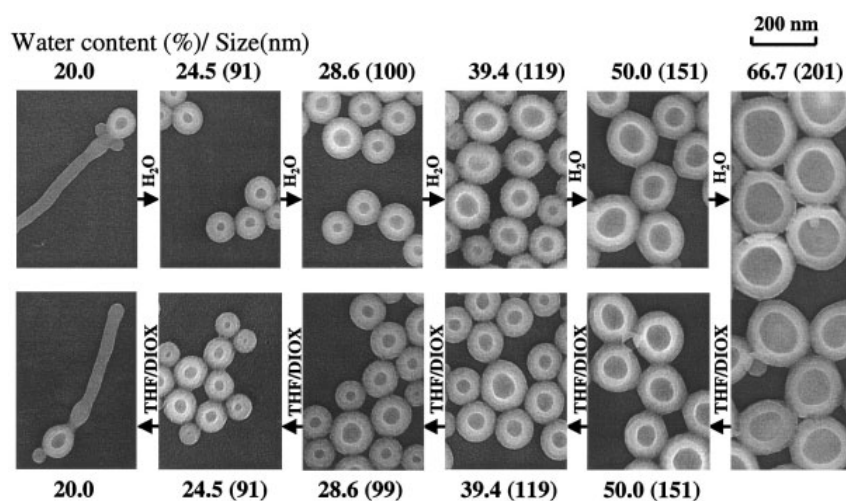


Figure 3.3. Reversibility of vesicle sizes in response to increasing or decreasing water contents for  $PS_{300}$ - $b$ - $PAA_{44}$  vesicles in a THF/dioxane (44.4/55.6) solvent mixture<sup>6,11</sup>.

In order to better understand the self-assembly of a given macromolecule in different conditions, phase diagrams become a most useful resource. This diagram describes what kind of structures are formed by the copolymer as a function of its composition and, when in solution, its concentration<sup>12</sup>.

Though very helpful, the obtention of a phase diagram for a new copolymer is a quite demanding task that requires much time and material to be performed. Given the scope of the work herein described (section 1.3: Scope of the project), we decided to concentrate our study on aqueous solutions with concentrations in the dilute aqueous regime ( $C \leq 1 \text{ mg.mL}^{-1}$ ), which confers an isotropic characteristic to the copolymer solution.

### 3.2. Charged Block Copolymers

The existence of charges in block copolymers brings more environmental responsiveness to the self-assembling material, since ionic strength and pH of the medium will affect the solubility of the polymeric chains<sup>13</sup>. Due to the complex interactions between polymeric chains, solvent and counter ions the self-assembling process for charged copolymers becomes more convoluted and, depending on the composition of the copolymer, also more dynamic.

This new element will affect the morphology of the self-assembled structures that can be achieved by the copolymers in dilute solution, ranging from core-shell micelles to multilayer structures, such as higher order vesicular structures<sup>14</sup> or lamellar vesicles<sup>11</sup> (figure 3.4).

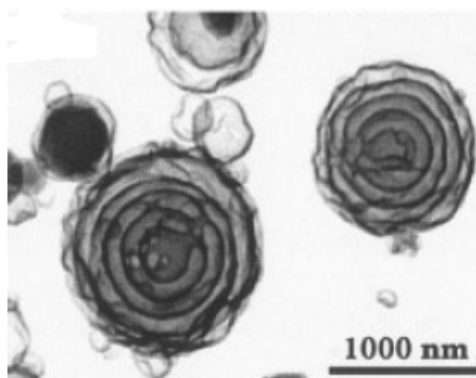


Figure 3.4. Hollow concentric vesicles from  $\text{PS}_{132}\text{-}b\text{-PAA}_{20}$ .

### 3.3. Polymer-modified Oligonucleotides<sup>15</sup>

Oligonucleotide-based block copolymers may have the ability to self-assemble in solution depending on the chemical composition of the block linked to the oligonucleotide. The intrinsic chemical incompatibility between the two blocks will induce the formation of self-assembled structures in solution. This behavior will be the more pronounced if the oligonucleotide is coupled to a hydrophobic polymer<sup>16-17</sup>.

Poly(butadiene)s are very hydrophobic polymers and present very low solubility in water. The high degree of 1,4 polymerization of the PBs provided by Prof. Axel Müller gives the polymers a very low  $T_g$  (approximately  $-100^\circ\text{C}$ )<sup>18</sup>. This is an advantageous property for self-assembly, as the dynamics of the system is not hindered by the formation of frozen structures<sup>19</sup>.

It is also important to remember that the vinyl groups pending from the main chain are the main responsible for the cross-linkability of poly(butadiene). Even if the polymer present high 1,4-polymerization, a certain number of vinyls will still be present on the macromolecule, allowing its cross-linkage.

Since the self-assembled structures are driven and held together only by non-covalent interactions, the ability to reinforce the mechanical strength of these structures by cross-linkage may become a very interesting property.

The study of the polymer-modified oligonucleotides self-assembly in dilute aqueous solution was performed by dissolution of the material in water (in a first approach) and in two different buffers: phosphate buffer saline, PBS (pH 7.4, Sigma) and in tris-EDTA, TE buffer containing 50 mM NaCl, which shall be called TE+NaCl buffer from this point onwards. Sodium chloride was added to the storage TE buffer in order to increase its ionic strength, which helps in the stabilization of the self-assembled structures by screening of the electrostatic interactions between the charges present on the backbone of the oligonucleotide.

These solutions with different composition were used to observe the effect of the ionic aqueous environment on the self-assembly of the nucleotide-based block copolymers. Though not having similar compositions both solutions contained only monovalent cations ( $\text{Na}^+$  and  $\text{K}^+$ ) in different concentrations and were used in order to perform preliminary studies on the self-assembly of polymer-modified oligonucleotides in dilute aqueous solution.

The samples used in the physical-chemical analyses were prepared in two different ways, according to the length of the PB segment linked to the oligonucleotide and, therefore, the synthetic method used. The copolymers synthesized by solid phase chemistry by direct dissolution of the dry oligonucleotide-based block copolymer in the appropriate solution. Ideally, after being re-suspended, the solid is vortexed for a couple of minutes and left overnight for complete re-suspension.

The copolymers obtained by heterogeneous chemistry were first dissolved in a small volume of tetrahydrofuran, THF and then slowly added to the buffer, dropwise, under stirring. After addition of the solution, the THF was removed from the mixture by rotoevaporation. No extrusion was performed in the sample preparation by either of the methods.

Determination of the concentration of the samples was not very straightforward, as the amount of material obtained after synthesis was generally quite small (~1-2 mg). The alternative methods to measure the concentration, such as UV spectroscopy for optical density measurements were not very accurate either due to the scattering effect of the samples or too low concentration. Therefore, in order to standardize the non-concentration dependent measurements, normalized concentrations based on the dilution obtained after SEC were used instead of using absolute concentrations.

Considering that the oligonucleotide-base block copolymers self-assemble into non-frozen, dynamic structures, reinforcement of the mechanical properties of the self-assembled structures should prove advantageous for applications in which stability of the self-assembly structures are necessary, such as in biological imaging technologies<sup>20</sup>. The “freezing” of the system could be obtained by cross-linking the PB blocks that constitute the hydrophobic part of the self-assemblies<sup>21</sup>.

Mechanical reinforcement was obtained by two different methods, depending on whether the self-assembled structures were in solution or deposited onto a surface. In solution, the nucleotide-based copolymers were exposed to UV irradiation ( $\lambda = 280$  nm) for 30 min. If the cross-linking was to be performed on the self-assemblies immobilized onto a surface, the exposure time was reduced to 5 min in order to minimize possible structural damages suffered by the oligonucleotide sequences during the process.

Characterization of the self-assembled structures was performed in order to determine both their dimensions and morphology. Dynamic Light Scattering, DLS was the chosen technique to investigate the hydrodynamic of the self-assemblies while Transmission Electron Microscopy, TEM, Atomic Force Microscopy, AFM, Confocal Laser Scanning Microscopy, CLSM and Scanning Electron Microscopy, SEM were used to assess their morphology.

### 3.3.1. Size Determination

Dynamic Light Scattering measurements were done in order to determine the hydrodynamic radius,  $R_h$  of the polymer-modified oligonucleotides self-assemblies in solution. In order to determine the dimensions of these structures, a time correlation function decaying in time was used<sup>22</sup>.

By performing several measurements at a finite number of angles and concentrations, the cooperative diffusion coefficients,  $D_m$  were calculated for each concentration. By extrapolation of the  $D_m$  values to zero concentration, the diffusion coefficient  $D_0$  is obtained, from which  $R_h$  can be calculated using the Stokes-Einstein equation<sup>21,22</sup> (equation 1):

$$R_h = \frac{kT}{6\pi\eta_0 D_0} \quad (1)$$

Where  $k$  is the Boltzmann constant,  $T$  is the temperature and  $\eta_0$  is the viscosity of the solution.

The self-assemblies were considered to be spherical in order to simplify the equations necessary for the calculation of the  $R_h$ . The veracity of this assumption would be supported by the existence of a single diffusive time in the correlation functions obtained in the DLS measurements and further confirmed by imaging techniques.

DLS measurements showed best correlations when the oligonucleotide-based copolymers were dissolved in buffer solution, either PBS or TE+NaCl. In water, the correlation function obtained in the DLS measurements shows two different correlation times. This could either indicate that the self-assembled structures are not spherical or the existence of different populations in the sample, with different

diffusive times. In order to verify these hypotheses, TEM imaging was performed on the  $C_{12}$ - $b$ -PB<sub>2000</sub> sample and will be discussed further on.

The measurements performed in buffer solutions were reproducible, with scattering intensity always kept in the range of 100-500 kHz in order to obtain accurate results. The polydispersity index measured by DLS was reasonable, varying from 0,1 to 0,3 depending on how diluted the solutions were.

The curves showing the diffusion coefficient as a function of the concentration obtained for each of the copolymers in PBS buffer and TE+NaCl buffer are depicted below (figures 3.5 and 3.6, respectively).

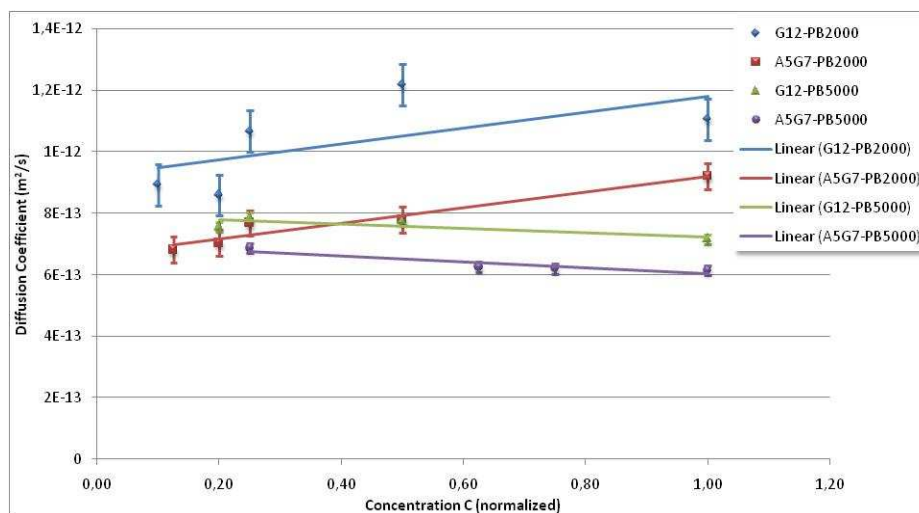


Figure 3.5. Diffusion coefficient as function of concentration for various polymer-modified oligonucleotides in TE+NaCl buffer at 300 K.

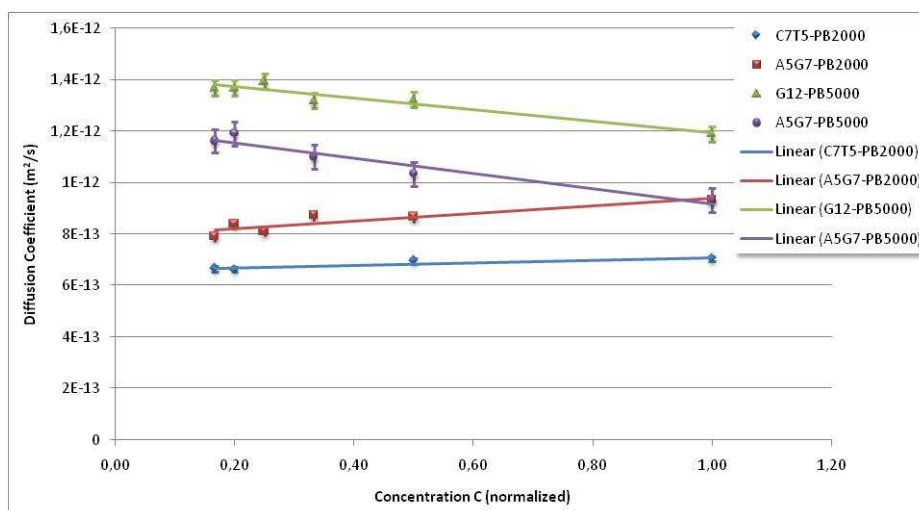


Figure 3.6. Diffusion coefficient as function of concentration for various polymer-modified nucleotide sequences in PBS buffer at 293 K.



The relation between the diffusion coefficients and the normalized concentrations for every of the nucleotide-based block copolymers is linear, falling in the range of the calculated error, leading to very good linear correlations.

The measurements of the samples prepared in PBS were performed at 293 K, whereas those in TE+NaCl buffer were done at 300 K. This difference in temperature was merely due to different temperature control settings for the equipments with which the measurements were performed and the effects of this change were taken in account for the calculation of  $R_h$ .

According to equation 1, this modification in the measurement conditions, namely the increase in temperature and the consequent reduction in viscosity, would induce an increase in  $R_h$ . The viscosity of the solutions was considered to be that of pure water.

The hydrodynamic radii obtained for each of the oligonucleotide-based copolymers, both in PBS and in TE+NaCl buffer, are shown in tables 3.1 and 3.2, respectively. Various conclusions could be drawn from the values obtained for the hydrodynamic radius of the copolymers in solution.

Copolymer	$D_0$ ( $m^2/s$ )	$R_h$ (nm)	$\Delta R_h$ (nm)	Error (%)
<b>G<sub>12</sub>-b-PB<sub>2000</sub></b>	$9,23 \cdot 10^{-13}$	232	38	16
<b>A<sub>5</sub>G<sub>7</sub>-b-PB<sub>2000</sub></b>	$6,64 \cdot 10^{-13}$	322	46	14
<b>G<sub>12</sub>-b-PB<sub>5000</sub></b>	$7,92 \cdot 10^{-13}$	270	11	4
<b>A<sub>5</sub>G<sub>7</sub>-b-PB<sub>5000</sub></b>	$7,02 \cdot 10^{-13}$	305	15	5
<b>A<sub>5</sub>G<sub>7</sub>-b-PB<sub>10000</sub></b>	$5,50 \cdot 10^{-13}$	389	109	28

Table 3.3. Hydrodynamic radius,  $R_h$  of the polymer-modified oligonucleotides in PBS buffer.

Copolymer	$D_0$ ( $m^2/s$ )	$R_h$ (nm)	$\Delta R_h$ (nm)	Error (%)
<b>A<sub>5</sub>G<sub>7</sub>-b-PB<sub>2000</sub></b>	$7,93 \cdot 10^{-13}$	325	21	6
<b>C<sub>7</sub>T<sub>5</sub>-b-PB<sub>2000</sub></b>	$6,58 \cdot 10^{-13}$	392	13	3
<b>G<sub>12</sub>-b-PB<sub>5000</sub></b>	$1,42 \cdot 10^{-12}$	182	9	5
<b>A<sub>5</sub>G<sub>7</sub>-b-PB<sub>5000</sub></b>	$1,21 \cdot 10^{-12}$	212	18	9

Table 3.4. Hydrodynamic radius,  $R_h$  of the polymer-modified oligonucleotides in TE+NaCl buffer.

The diffusion coefficients, as a function of the concentration, for polymer-modified oligonucleotides of similar PB lengths follow parallel linear trends. This indicates that the size of the self-assembled structures seems to depend on the composition of the oligonucleotide composing the copolymer.

Given that the oligonucleotides used in the synthesis of each of these copolymers contain the very same amount of bases (12 nucleotides), it becomes clear that the composition of the oligonucleotide is the variable that defines the size of the self-assembled structures.

The conformation acquired by the oligonucleotides will depend both on their interaction with the medium, because of the charges present along the backbones and the ones that may be present in the solution, and on the intra- and intermolecular interactions between the oligonucleotides within the self-assembly, mainly considering the formation of H-bonds.

It is known that oligonucleotide sequences containing a repeat number of guanosines (G) generate, in solution, a secondary structure in the form of a quartet, G-quartets (figure 3.7), based on intermolecular formation of H-bonds between the guanosines<sup>23</sup>. The formation of these structures is assumed to be driving the decrease in size of the self-assemblies from the copolymers containing the oligonucleotide G<sub>12</sub> in comparison with the other sequences, since the G-quartets are more compact than other nucleotide combinations. Nevertheless, in order to confirm this hypothesis, accurate Circular Dichroism, CD spectroscopy measurements still need to be performed.

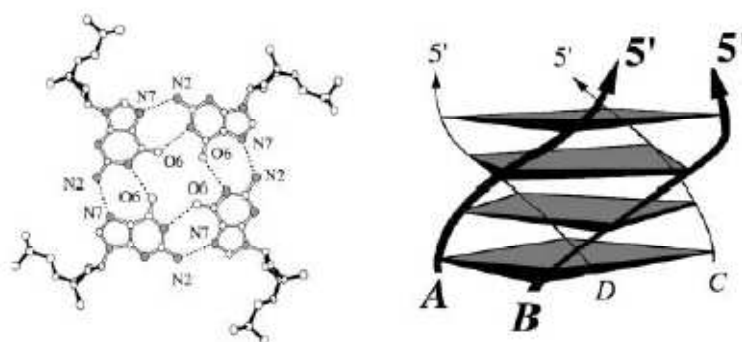


Figure 3.7. Tridimensional structure of G-quartets<sup>23</sup>.

The size change induced by the substitution of five of the guanosines in the oligonucleotide by adenosines, in such a way that the statistical sequence does not contain many sequential guanosines, is significant and quite clear. This substitution leads to a size modification of 39% for the oligonucleotides modified with PB<sub>2000</sub> and approximately 15% for those modified with PB<sub>5000</sub>.

It is important to notice that even considering the error in the  $R_h$  calculated for each of the polymer-modified oligonucleotides, the size ranges do not overlap, which further confirms that the size variation is actually a result of the modification in the oligonucleotide sequence composition.

The reason why the size modification is more drastic in the copolymers containing  $PB_{2000}$  is because this polymer is shorter than  $PB_{5000}$ , which leads to a more pronounced change in the cross-area of the copolymeric molecules<sup>24</sup>. This effect will lead to a reduction in the dimensions of the self-assembled structures.

The effect of concentration of cations in the aqueous milieu on the size of the self-assembled structures can also be observed on the self-assembly of the  $PB_{5000}$ -modified oligonucleotides. The reduction in the  $R_h$  observed for the copolymers measured in TE+NaCl buffer amounts to approximately 30% of the radius in PBS, which is an effect of the screening of the electrostatic interactions between the charges on the oligonucleotide backbone by the ions in the buffer.

As the concentration of positively charged ions of the PBS buffer is higher than the one of TE+NaCl, the screening of electrostatic interactions between the charges along the oligonucleotides is more effective, thus reducing the excluded volume of the molecule and leading to a behavior that tends to resemble neutral macromolecules<sup>25</sup>. This effect induces a stretching of the oligonucleotides, increasing their length and allowing a denser packing of the copolymer in the self-assembly. In TE+NaCl buffer, the screening is not so efficient. Therefore the reduction in size is due to the larger excluded volume of the molecules in the self-assembled structures, in agreement with the diffusion coefficients observed for polyions, which increases with the reduction of the salt concentration in the solution<sup>25</sup>.

In the analysis of the DLS data of  $A_5G_7$ -*b*- $PB_{2000}$  the same effect was not observed, since the copolymer presented a similar radius both in TE+NaCl and in PBS buffer. Considering that the measurements were performed at different temperatures and that the size of copolymer makes it even more susceptible to environmental changes, due to the ratio between the hydrophobic and the hydrophilic blocks, it is possible that the ionic strength effects were masked.

It is also important to remember that DLS is only able to calculate the radius of the self-assembled structures, based on the equations and mathematical models used in the calculations. Even so, calculation of the gyration radius,  $R_g$  by Static Light Scattering, SLS could not be performed due to the impossibility to determine exact

solution concentrations. As a consequence, the shape factor  $\rho$  ( $R_g/R_h$ ) could not be obtained<sup>22</sup>.

The hydrodynamic radius represents the size of the self-assembled structures taking in account the swelling and the charges effect, having, therefore, a bigger value than that obtained for the radius of gyration. The latter would provide a more accurate calculation of real size of the self-assemblies, although both values should be in the same order of magnitude<sup>22</sup>.

In order to resolve the morphological properties of oligonucleotide-based copolymers self-assemblies, different microscopy techniques were employed.

### 3.3.2. Morphological Studies

The determination of the morphology of the polymer-modified oligonucleotides was investigated by different microscopy techniques, namely, TEM, AFM, CLSM and SEM.

Firstly, TEM measurements were performed to observe the self-assembled structures formed by the copolymers in water. The sample was prepared for analysis on a coated copper grid (chapter 6: Materials and Methods) without staining. The micrographs obtained showed spherical structures in two different size ranges, which confirmed the hypothesis raised by the analysis of the DLS measurements.

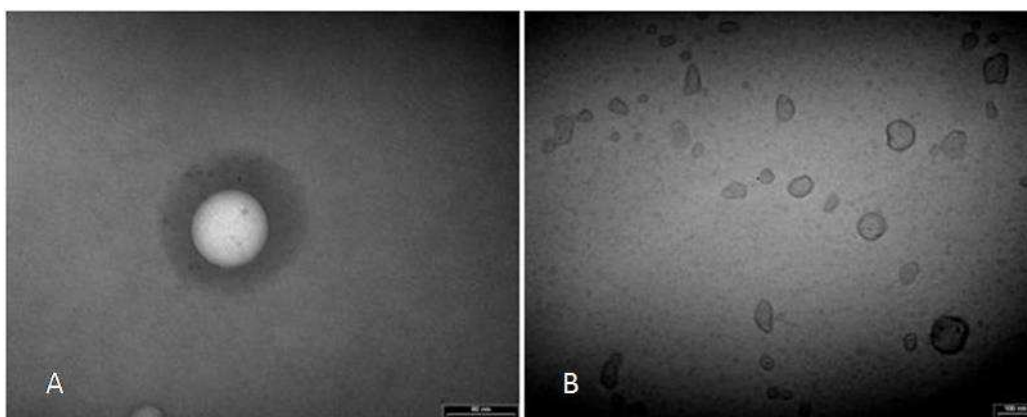


Figure 3.8. TEM micrographs of the small self-assembled structures of  $C_{12}$ -*b*-PB<sub>2000</sub> in water: A - Water-filled vesicle and B - empty vesicles.

One of the populations had a diameter in the range of 60-80 nm, as observed in the TEM micrographs (figure 3.8). This size range is much smaller than that observed for the self-assembled copolymers in buffer. This is due to the inexistence

of counterions in the medium, which, in agreement with what was previously discussed, leads to higher diffusion coefficients and, therefore, to smaller sizes.

The existence of a rim around the structures observed in the micrographs clearly indicates that the self-assembly process of  $C_{12}\text{-}b\text{-PB}_{2000}$  in dilute aqueous solution leads to the formation of vesicles, in which the PB would form the inner layer of the membrane while the oligonucleotides would be exposed to the solution and to the inner aqueous pool of the structure. The fact that the inner part of the vesicle on figure 3.8-A appears to be lighter than the background suggests that the structure could still be filled with water. This would support the self-assembly into vesicular structures. Despite the fact that no staining agent was used, the high contrast observed at the rim of the vesicles on figure 3.8-B is due to the phosphorus atoms of the nucleotide sequences, which gives more contrast to the image upon exposure to the electron beam<sup>17</sup>.

The second population observed in the TEM pictures was composed of larger structures, in the range of 1-2  $\mu\text{m}$ , formed by the arrangement of these smaller vesicles into more complex structures, such as the ones previously observed with charged copolymers<sup>6</sup>. These Higher Order Vesicular structures, HOVs (figure 3.9), correspond to what was observed in the DLS measurements of the polymer-modified oligonucleotides and clearly show the existence of smaller vesicles aggregated into larger ones.

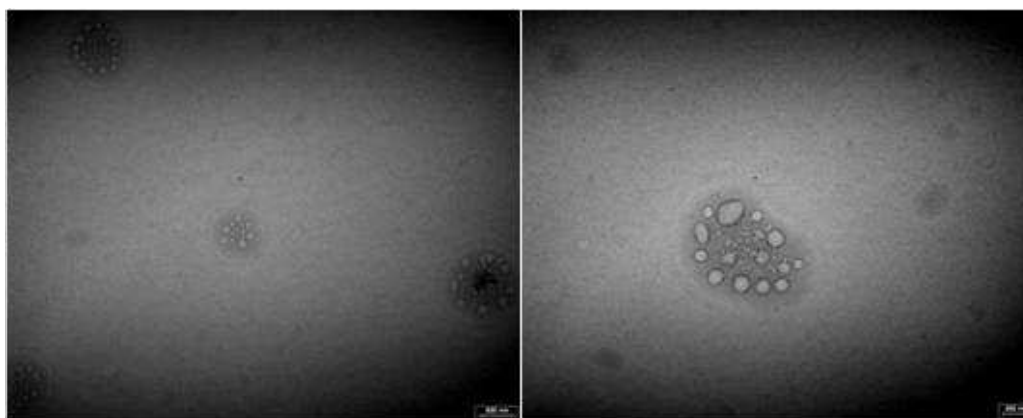


Figure 3.9. TEM micrographs show the Higher Order Vesicular structures, HOVs formed by  $C_{12}\text{-}b\text{-PB}_{2000}$  in water.

The exchange of water for buffer in preparation of the oligonucleotide-based copolymers samples modifies the thermodynamics of the self-assembling process in solution. TEM imaging of the samples in buffer does not show the formation of any HOVs (figure 3.10). This is a result of the screening of the electrostatic interactions

between charges along the oligonucleotide backbones, which stabilizes the copolymer, reducing its excluded volume, and yields the formation of more homogeneous self-assembled structures.



Figure 3.10. TEM micrograph of unstained  $A_5G_7$ - $b$ - $PB_{5000}$  in PBS buffer, showing only single vesicles.

Further analyses of the oligonucleotide-based copolymer self-assembly induced in water were performed by AFM measurements, in a collaborative project with the group of Dr. Gunter Reiter (Freiburg, Germany). First, the self-assembled copolymer was deposited onto mica from a 10x diluted solution from the normalized stock solution and then evaporated. The analysis of the micrographs obtained showed large vesicles (510 nm) deposited onto the surface as well as some smaller ones (100 nm) (figure 3.11).

The size range of the vesicles observed both in TEM and AFM analyses is approximately the same. The rim of the vesicles is very clear, reconfirming their morphology. Because of the drying process to which the vesicles were submitted, they lose their structural integrity, opening and releasing the water contained in their inner pool. What can be observed on the micrograph are only broken structures, reason why the vesicular membrane is so sharp.

In order to obtain more stable self-assemblies, the polymer-modified oligonucleotide sample was submitted to a cross-linking process, in which the PB molecules present in the inner layer of the membrane formed cross-linked bonds between themselves, conferring mechanical strength to the vesicles.

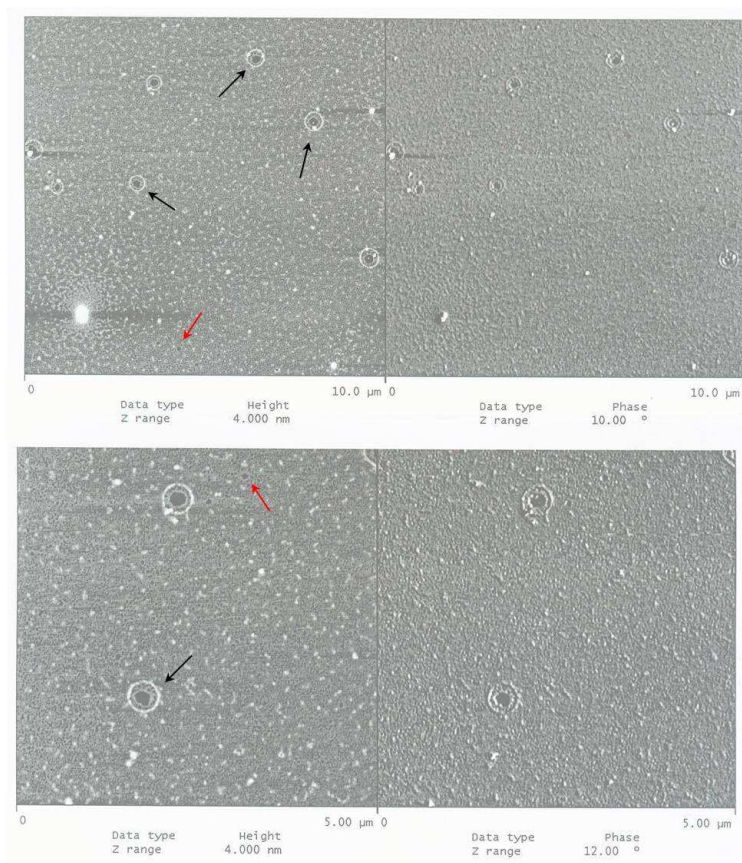


Figure 3.11. AFM micrograph of  $C_{12}$ - $b$ - $PB_{2000}$  on mica, showing large vesicular structures (black arrows) and some small ones (red arrows) present on the mica surface.

AFM measurements were performed on silicon wafers by drop evaporation of a dilute solution (0.001%) of the cross-linked copolymer. The micrographs obtained show the formation of dendritic structures, composed by the self-assembled vesicles previously observed both by TEM and AFM (figure 3.12). These vesicles are now more stable than before, as they retain the spherical shape even in dry conditions. Why these dendrites are formed is still a matter of discussion, but the oligonucleotides seem to drive the formation of these structures onto the silicon wafers, possibly due to the fact that they possess a certain degree of crystallinity.

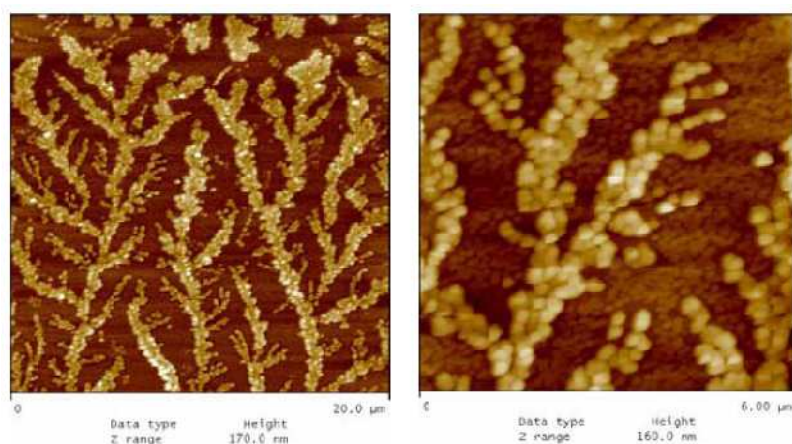


Figure 3.12. AFM micrographs showing dendritic structures formed by the self-assembled  $C_{12}$ -*b*-PB<sub>2000</sub> on a silicon wafer.

Similar structures were also observed in TEM measurements (data not shown), though it was not clear in those analyses that the dendrites were composed by these self-assembled vesicles.

Two-color CLSM analyses were subsequently performed to find further morphological evidence to support the self-assembly of the oligonucleotide-based block copolymer into vesicles<sup>16</sup>. In order to do so, the copolymer was stained with two different dyes: Bodipy<sup>®</sup> 630/650-Xt (Invitrogen) was used to label the hydrophobic PB layer while the chelating agent Syto9<sup>®</sup> (Invitrogen) stained the oligonucleotide strands (figure 3.13).

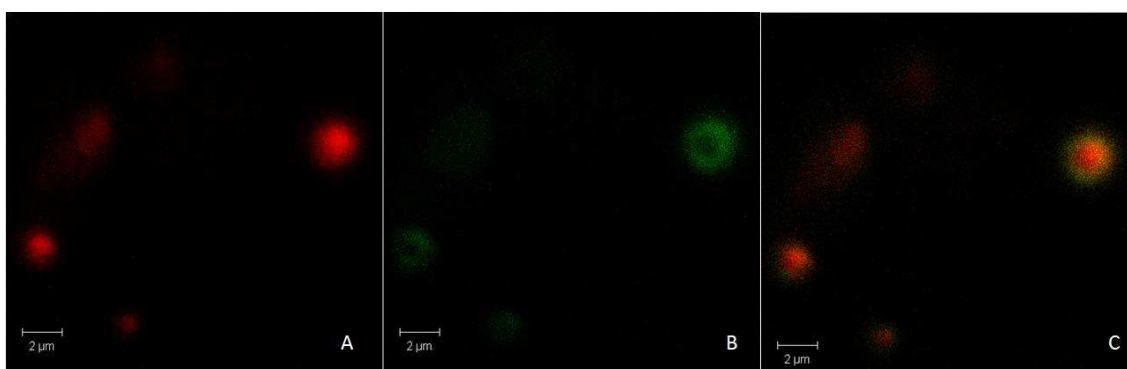


Figure 3.13. Two-color CLSM micrographs of  $C_{12}$ -*b*-PB<sub>2000</sub> showing: A - the hydrophobic part of the structure labeled with Bodipy<sup>®</sup>; B - the oligonucleotides on the shell of the vesicles chelated with Syto9<sup>®</sup> and C - the colocalization of the signals on the self-assembled structures<sup>16</sup>.

The staining with Bodipy<sup>®</sup> was performed by addition of a 100 nM solution of the dye in DMSO to the aqueous solution of the polymer-modified oligonucleotide.



Due to its hydrophobicity, the dye is entrapped in the poly(butadiene) layer of the self-assembled structures, which, then, becomes fluorescent (figure 3.13-A). The labeling with Syto9<sup>®</sup> was adapted from a common “Life/Dead” assay used in biology to stain the genomic DNA of bacteria. The staining agent chelates the oligonucleotides forming the outer rim of the vesicles that now shine upon excitation (figure 3.13-B).

Through two-color CLSM measurements both the hydrophobic and hydrophilic parts of the structures could be observed at the same time. The homogeneous colocalization of the two fluorescence signals (figure 3.13-C), indicates that the particles consist of a complex organization of vesicular structures, with a size range of 1-2  $\mu\text{m}$ . The shiny oligonucleotide shells surrounding the core of the structures indicate that the HOVs consist of multi-vesicles encapsulated in one large vesicle. The micrometer-sized fluorescent structures detected by fluorescence microscopy correspond to the larger population of the nucleotide-based copolymer previously observed by TEM and AFM. Due to the detection limits of the technique, the smaller vesicles could not be identified.

SEM imaging was eventually performed to resolve the morphology of the self-assembled structures in PBS buffer, prior and after reticulation of the hydrophobic polymer segments, and in TE+NaCl buffer (figure 3.14).

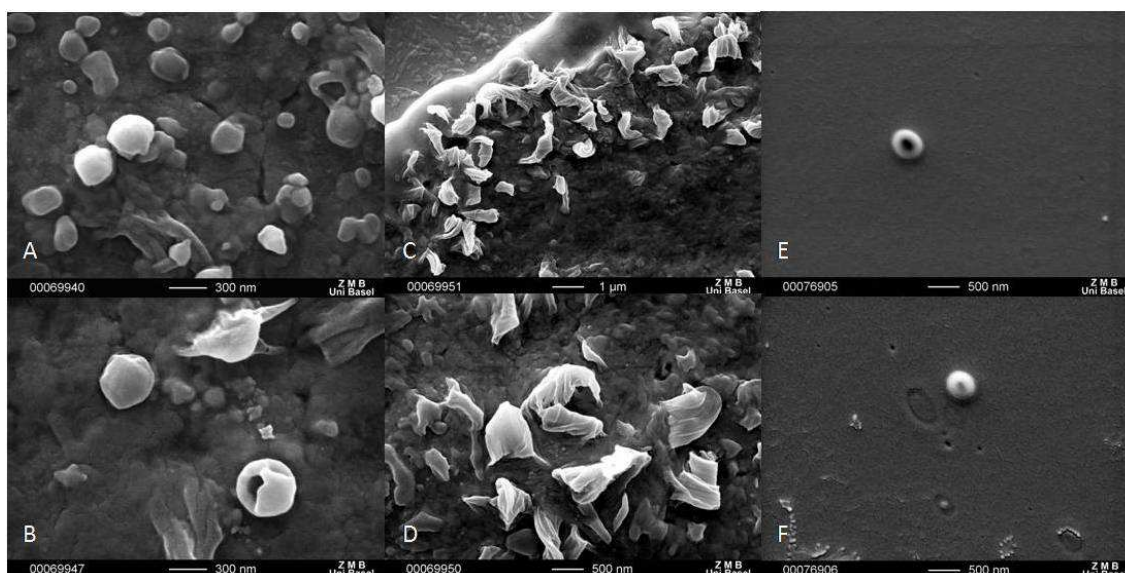


Figure 3.14. SEM micrographs of polymer-modified oligonucleotides: A-B - UV reticulated sample of  $G_{12}$ - $b$ - $PB_{2000}$  in PBS, C-D - non-reticulated sample of  $G_{12}$ - $b$ - $PB_{2000}$  in PBS and E-F - $C_7T_5$ - $b$ - $PB_{2000}$  in TE+NaCl buffer.

The reticulation of the PB layer was once again performed by UV-induced cross-linking polymerization to further reinforce the mechanical stability of the vesicles. The preparation of the SEM samples will be further discussed (Chapter 6: Materials and Methods).

Micrographs 3.14-A to -D show the same self-assembled polymer-modified oligonucleotide,  $G_{12}$ -*b*-PB<sub>2000</sub>, in PBS, reticulated (-A and -B) and non-reticulated (-C and -D). The structures observed in Figure 3.14-A and -B are in agreement with the self-assembly of the nucleotide-based copolymer into vesicular structures.

The micrographs show that the morphology of the self-assembly is solely preserved in vacuum. One can observe in figure 3.14-B a broken vesicle, showing the inner cavity of its structure upon evaporation of the solution from its aqueous pool. The reticulation process confers solid-like properties to the otherwise fluid polymer membrane of the vesicles. SEM measurements also reveal, in average, good correlation of the size compared to that calculated through DLS (table 3.1), which was not expected considering that the self-assembled structures are submitted to vacuum in order to perform the measurement.

In figure 3.14-C and -D membrane-like structures can be observed. These are the result of the disassembling process (bursting) of the vesicular structures due to the environmental conditions to which they were submitted to during the sample preparation for SEM. The osmotic stress induced by washing steps with doubly-distilled water to remove salts and non-adhering material from the grid caused the disintegration of the self-assembly, leaving behind only the broken membranes. This reinforces and confirms the assumption that reticulated self-assemblies gained mechanical resistance via the cross-linking process.

Figure 3.14-E and -F correspond to a sample of the polymer  $C_7T_5$ -*b*-PB<sub>2000</sub> in TE+NaCl buffer. Though not cross-linked, the vesicular structures formed by the copolymer in buffer survived the sample preparation and remained intact during the SEM measurement. This is due to the fact that the ionic strength of the buffer is not as high as that of PBS, inducing less osmotic pressure on the vesicles and allowing them to retain their shape.

One can observe in the micrographs that the central part of the vesicles is darker, which indicates that they are still filled. Once again, the size of the structures observed are similar to those obtained by DLS (table 3.2).

Micrometer scales structures were also observed, but only in very specific conditions. One sample of the copolymer  $A_5G_7-b-PB_{2000}$  was prepared in PBS buffer and stored at room temperature for a month, in order to observe whether there was any time-related variable in the self-assembling process. SEM imaging showed that HOVs were formed in this sample (figure 3.15).

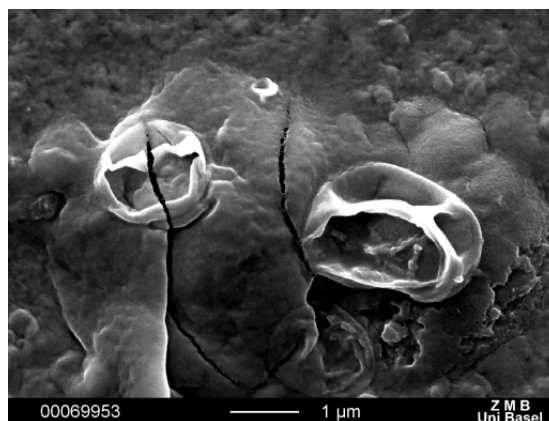


Figure 3.15. SEM image of HOVs formed by the copolymer  $A_5G_7-b-PB_{2000}$  in PBS after long time periods.

This leads us to believe that the effect of the ionic strength on the self-assembly of the polymer-modified oligonucleotides is, in the short term, to slow down the formation of these structures, which still tend to be achieved by the copolymer after long times periods.

### 3.4. References

1. Davis, F.J. *Polymer Chemistry: A Practical Approach*; Oxford University Press: Oxford, UK, 2004.
2. Hamley, I.W. *Introduction to soft matter: synthetic and biological self-assembling materials*; John Wiley and Sons, Inc.: New York, NY, USA, 2007.
3. Solomons, T.W.G.; Fryhle, C.B. *Organic Chemistry*, 7<sup>th</sup> Edition; John Wiley and Sons, Inc.: New York, NY, USA, 2000.
4. Branden, C.; Tooze, J. *Introduction to Protein Structure*, 2<sup>nd</sup> Edition; Garland Publishing: New York, NY, USA, 1999.
5. Watson, J.; Crick, F. Molecular Structure of Nucleic Acids – A Structure for Deoxyribose Nucleic Acid *Nature*, **1953**, 171, 737–738.
6. Discher, D. E.; Eisenberg, A. Polymer Vesicles. *Science*, **2002**, 297, 967-973.

7. Deschamps, A.A.; Grijpma, D.W.; Feijen, J. Poly(ethylene oxide)/ poly(butylene terephthalate) segmented block copolymers: the effect of copolymer composition on physical properties and degradation behavior. *Polymer*, **2001**, *42*, 9335-9345.
8. Ikkala, O.; ten Brinke, G. Functional Materials Based on Self-Assembly of Polymeric Supramolecules. *Science*, **2002**, *295*, 2407 - 2409
9. Kriksin, Y.A.; Erukhimovich, I.Y.; Khalatur, P.G.; Smirnova, Y.G.; Brinke, G. Nonconventional morphologies in two-length scale block copolymer systems beyond the weak segregation theory. *J. Chem. Phys.* **2008**, *128*, 244903.
10. Battaglia, G. and Ryan, A. J. The evolution of vesicles from bulk lamellar gels. *Nature Materials*, **2005**, *4*, 869 - 876.
11. Soo, P. L. and Eisenberg, A. Preparation of block copolymer vesicles in solution. *J. Polym. Sci. Part B: Polym. Phys* **2004**, *42*, 923-938.
12. Koningveld, R.; Stockmayer, W.H.; Nies, E. *Polymer Phase Diagrams – A Textbook*; Oxford University Press: Oxford, UK, 2001.
13. Stuart, M.A.C.; Hofs, B.; Voets, I.V.; de Keizer, A. Assembly of polyelectrolyte-containing block copolymers in aqueous media. *Curr. Opin. Colloid Interface Sci.* **2005**, *10*, 30-36
14. Geng, Y.; Ahmed, F.; Bhasin, N.; Discher, D.E. Visualizing Worm Micelle Dynamics and Phase Transitions of a Charged Diblock Copolymer in Water. *J. Phys. Chem. B* **2005**, *109*, 3772–3779.
15. Teixeira Jr., F.; Nussbaumer, M.; Syga, M.-I.; Nosov, S.; Müller, A.H.E.; Vebert-Nardin, C. Polymer-modified oligonucleotides: synthesis and characterization of biologically active self-assembled interfaces. *In preparation*.
16. Alemdaroglu, F.E.; Herrmann, A. DNA meets synthetic polymers - highly versatile hybrid materials. *Org. Biomol. Chem.* **2007**, *5*, 1311-1320.
17. Teixeira Jr., F.; Rigler, P.; Vebert-Nardin, C. Nucleo-copolymers: Oligonucleotide-based amphiphilic diblock copolymers. *Chem. Comm.* **2007**, *11*, 1130-1132.
18. Mark, J.E. *Polymer Data Handbook*; Oxford University Press: Oxford, UK, 1999.
19. Cameron, N.S.; Adi Eisenberg, A.; Brown, G.R. Amphiphilic Block Copolymers as Bile Acid Sorbents: 2. Polystyrene-b-poly(N,N,N-trimethylammoniummethylene acrylamide chloride): Self-Assembly and Application to Serum Cholesterol Reduction. *Biomacromolecules* **2002**, *3*, 124-132.
20. *Block Copolymers in Nanoscience*; Lazzari, M., Liu, G, Lecommandoux, S., Eds.; Wiley-VCH, Weinheim, Germany, 2006.

21. C. Nardin, T. Hirt, J. Leukel and W. Meier. Polymerized ABA Triblock Copolymer Vesicles. *Langmuir*, **2000**, *16*, 1035-1041.
22. Schmitz, K.S., *An introduction to Dynamic Light Scattering by Macromolecules*; Academic Press Limited, London, UK, 1990.
23. Stefl, R.; Cheatham, T.E.; Spackova, N.; Fadrna, E.; Berger, I.; Koca, J.; Sponer, J. Formation pathways of a guanine - quadruplex DNA revealed by molecular dynamics and thermodynamic analysis of the substates. *Biophys. J.* **2003**, *85*, 1787-1804.
24. Privalko, V.P. On the Molecular Packing Density in Crystalline Polymers. *Polym. J.* **1975**, *7*, 202-206.
25. *Physical Chemistry of Polyelectrolytes*; Radeva, T., Ed.; CRC Press, Danvers, MA, USA, 2001.

## Chapter 4: Biological Activity

## 4.1. Hybridization

Hybridization is a very selective process, inherent to DNA chains, through which nucleotide strands interact via the formation of specific H-bonds to assemble through Watson-Crick base-pairing<sup>1</sup>. The self-assembly of DNA is both composition and orientation dependant, only occurring by the formation of the H-bonds between the base pairs cytidine/guanosine and adenosine/thymidine along the two strands (figure 4.1), which will be combined in opposite orientations (3'-end to 5'-end).

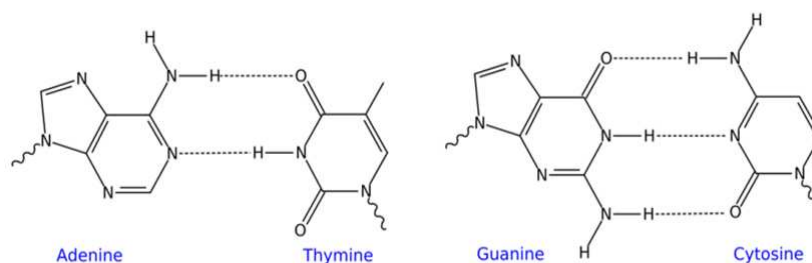


Figure 4.3. Base pairing between nucleic bases Adenine/Thymine and Cytosine/Guanine.

When the nucleic bases along the nucleotide strands are fully complementary, i.e., the sequence of oligonucleotides composing one of the strands corresponds exactly to the sequence of complementary oligonucleotides on the other strand, the self-assembly of the DNA occurs into a double helix (figure 4.2).

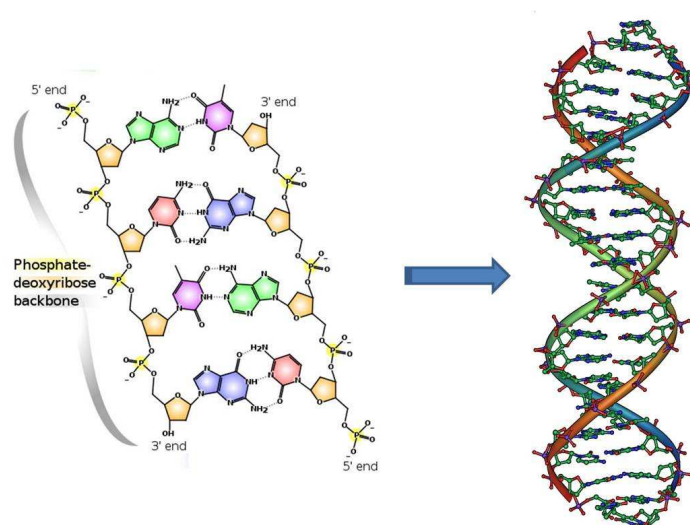


Figure 4.4. DNA self-assembly into a double helix by the formation of H-bonds between the complementary nucleotide sequences.

The hybridization process is well described, being dependant on several factors, such as temperature<sup>2</sup> and the presence of denaturing agents, such as urea<sup>3</sup>. In solution, the hybridization yield is generally 100% for fully complementary sequences. This yield maybe hindered in case the single strands have palindromic regions, i.e., can be read the same in both directions, allowing the sequences to fold onto themselves, forming structures known as hairpins or stem-loops (figure 4.3)<sup>4</sup>.

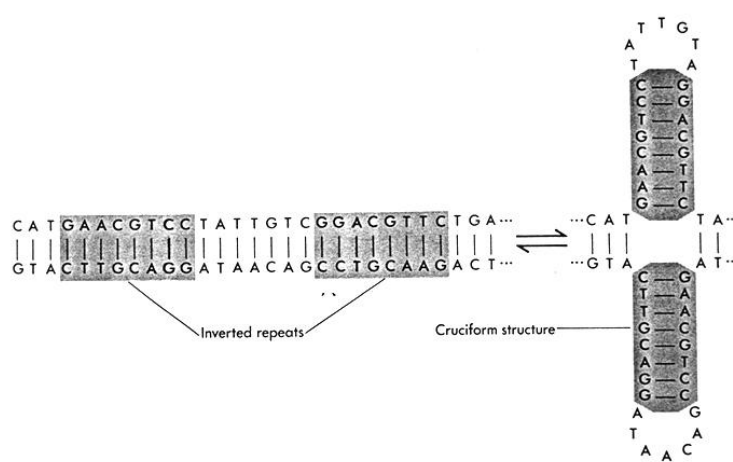


Figure 4.5. Formation of hairpins or stem-loops on DNA sequences containing palindromic regions.

This ability to self-assemble into a double stranded helix brings many possibilities for the use of oligonucleotides in medicinal chemistry. Other species, such as markers, labels or linkers, can be bound to one of the strands and immobilized in the system by the formation of the double helix<sup>5,6</sup>.

Similarly to charged<sup>7</sup> or peptide-based<sup>8</sup> copolymers, polymer-modified oligonucleotide sequences may also be used in the construction of stimuli-responsive key-lock systems, which will have temperature as triggering agent for the disassembly of the system.

In order to take advantage of the hybridization process in the oligonucleotide-based copolymeric systems, it is important to verify if any conformational changes in the nucleotide sequences took place as a result of the polymer modification. Concerns as to how much the polymer modification would affect the properties of the oligonucleotides were raised, as well as doubts regarding the bioactive conformation of the sequences upon self-assembly, given the dense packing of the oligonucleotides in the vesicular structure.

The hybridization process onto surfaces, which should be similar to the hybridization process of the sequences within the self-assembly, has been addressed theoretically<sup>9</sup>, although it has been used for some time now in different applications, such as the DNA chip technology<sup>10</sup>. More rigorous experimental studies are currently being performed in order to better understand the elements that influence the hybridization mechanism onto surfaces<sup>5</sup>.

#### 4.1.1. Oligonucleotide Configurational Analyses

To assess whether any change has occurred upon polymer modification, Circular Dichroism, CD spectroscopy was performed to verify the conformation of the nucleotide sequences along the amphiphilic macromolecules and in the self-assembled structures.

CD spectroscopy monitors the differential absorption of left- and right-handed circularly polarized light. This information allows the determination of the configuration of macromolecules, including the secondary structures of proteins and the handedness of nucleic acids.

The analyses were performed using several samples of the oligonucleotide-based block copolymer at different concentrations and a sample of non-modified oligonucleotide, as reference. The result of the CD measurements can be seen in figure 4.4.

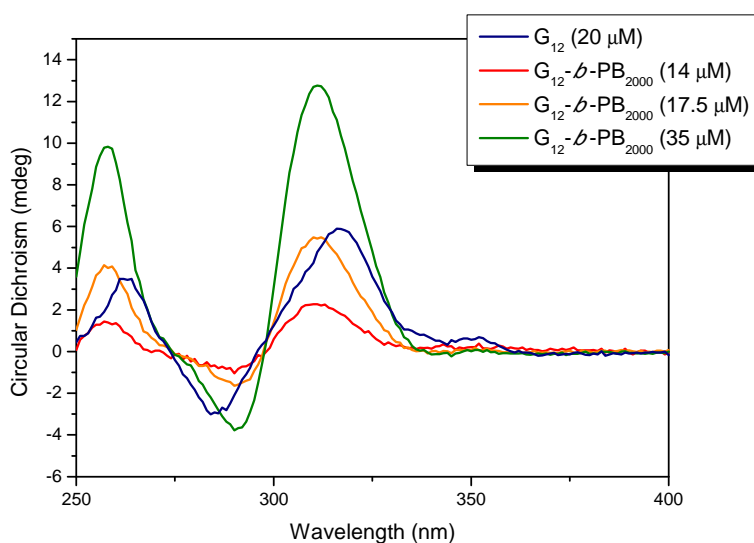


Figure 4.6. CD spectra of a 20  $\mu\text{M}$  water solution of  $G_{12}$  (—) and  $G_{12}$ - $b$ - $PB_{2000}$  in TE+NaCl buffer in the following concentrations: 14  $\mu\text{M}$  (—), 17,5  $\mu\text{M}$  (—) and 35  $\mu\text{M}$  (—).



The concentrations of the polymer-modified oligonucleotides used in these analyses were estimated from UV-Vis measurements performed at 260 nm and were calculated by comparison with the signal obtained for a known concentration of the non-modified oligonucleotide. It is important to remember that these values might not reflect the real concentration of the oligonucleotide-based copolymer, as they do not take in account the influence of PB or the shielding of the signal due to the self-assembly into vesicular structures.

The results of the measurements showed that the characteristic peaks of the oligonucleotide linked to the synthetic polymer did not suffer any major changes. The chiral centers and right-handedness observed in the spectra indicate that even after the polymer modification the oligonucleotides retain their A-form configuration, as it would be expected in the solution conditions used<sup>11</sup>. The slight difference between the shifts of the non-modified and the polymer-modified oligonucleotides arise from the fact that the non-modified sample was measured in water, leading to a transition between the A- and B-forms, both of which have the same handedness, but a different compactness<sup>11</sup>.

One can also observe the expected variation of the intensity of the signal as a function of the concentration of the sample, which is typical for UV-Vis spectroscopy.

These results confirm that the handedness of the oligonucleotide sequences present in the self-assembled vesicles was preserved after modification with poly(butadiene) and self-assembly. Therefore, these oligonucleotide sequences are still likely to undergo hybridization, even within the self-assembled structures, as no change in configuration was observed.

#### 4.1.2. Preliminary Hybridization Studies

Preliminary studies regarding the hybridization of the nucleotide-based block copolymers were performed, in order to observe the influence of the process on the self-assembly of the polymer-modified oligonucleotides.

Considering that hybridization takes place, a modification in the size and/or morphology of the self-assembled structures would be expected. This modification would be a result of the change in the molecular weight of the hydrophilic block and, therefore, the volume fraction between the hydrophobic and the hydrophilic blocks of

the oligonucleotide-based copolymers. This would also lead to the stiffening of the oligonucleotide shell, changing the rod-coil balance of the copolymer.

The hybridization process of the oligonucleotides within the self-assembled structures is comparable to the mechanism onto surfaces; one must consider the density of chains onto the surface to be very high, as the macromolecules must stay packed close together to maintain the structural stability of the self-assemblies.

The density of oligonucleotides in the self-assembled structure shell could be calculated by Static Light Scattering, SLS analysis, which due to the uncertainties regarding sample concentration was not performed. Despite the impossibility of calculating the molecular density onto the vesicles, one can have an idea of how dense this packing can be by considering that the self-assembled structures from the triblock poly(2-methyl-2-oxazoline)-*block*-poly(dimethylsiloxane)-*block*-poly(2-methyl-2-oxazoline), PMOXA-*b*-PDMS-*b*-PMOXA ( $M_n = 9000 \text{ g.mol}^{-1}$ )<sup>12</sup> have a surface molecular density of approximately  $6,12 \cdot 10^{12}$  molecules/cm<sup>2</sup>, which is very high when compared to the value calculated by Razumovitch et al. in order to obtain 100% hybridization<sup>13</sup>.

As the hybridization onto surfaces of polymer modified nucleotide sequences is still subject of studies and dependent on the density of oligonucleotide within the shell of the vesicles<sup>7</sup>, quantification of the hybridized sequences within the vesicles could not be made.

In order to stay consistent with the scope of this work (section 1.3), we performed only preliminary studies of hybridization of polymer-modified oligonucleotides within the self-assembled structures, using DLS and TEM to observe what structural changes occurred as a consequence of base-pairing.

Before undergoing hybridization, the oligonucleotide-based copolymers were dialyzed and lyophilized (Chapter 6: Materials and Methods). The complementary strand, probe, of the polymer-modified oligonucleotide, target, was dissolved in PBS at a concentration of 100  $\mu\text{M}$ . The solution of the probe was added to the target, and shaken for a couple of minutes. The probe solution had an excess of material, in order to saturate the system and allow maximum hybridization efficiency.

After shaking, the target/probe solution was heated up to 40°C for 5 min and then allowed to cool down slowly to room temperature over night. This heating step was performed because the temperature of 40°C is above the melting point of a 12-nucleotide long sequence. By heating up the sample any non-specific hybridization,

i.e., formation of incomplete double helices would be undone. Letting the system slowly cool down permitted the complete hybridization of the nucleotide strands.

After hybridization, the target/probe solution was submitted to an aqueous SEC, in order to separate the now hybridized self-assembled structures from the non reacted probe sequences (figure 4.5). Sepharose 2B was used as chromatographic bed and the eluent solution used was PBS.

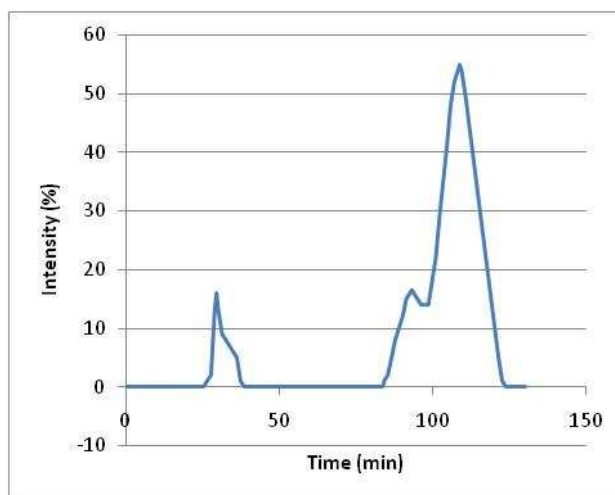


Figure 4.7. SEC chromatogram for the polymer-modified oligonucleotide  $G_{12}$ - $b$ - $PB_{2000}$  hybridized with its complementary sequence,  $C_{12}$ .

By analysis of the chromatogram one can observe that the separation between the free oligonucleotide and the hybridized, self-assembled oligonucleotide-based copolymer was very efficient. The chromatogram also shows broadening of the first peak, related to the hybridization of the oligonucleotide-based copolymers within the vesicular shell. As intervesicular bonding is not possible, given that hybridization is a highly orientation dependant process, this could indicate that the hybridization of the self-assembled structures was not homogeneous, yielding more polydisperse self-assemblies than those observed for the non-hybridized copolymer.

Dynamic Light Scattering was then performed to evaluate whether there were any modification in the size of the self-assemblies upon hybridization. As previously described (section 3.3.1), DLS measurements were done to determine the  $R_h$  of the self-assembled structures by using a time-decaying correlation function.

The diffusion coefficient  $D_0$  was calculated at 293 K for two different hybridized oligonucleotide-based copolymer samples in PBS, namely,  $A_5G_7$ - $b$ - $PB_{2000}$ + $C_7T_5$  and

$G_{12}$ -*b*-PB<sub>2000</sub>+C<sub>12</sub> (figure 4.6). Sample preparation was done according to what was previously described.

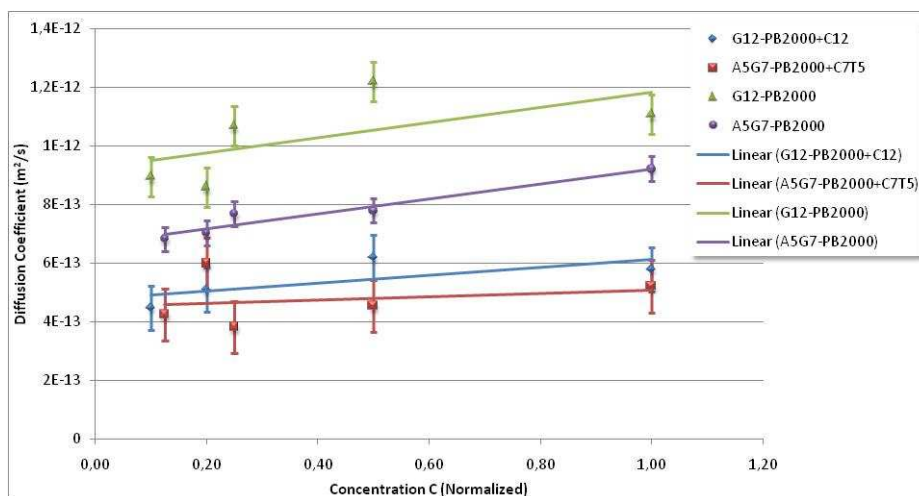


Figure 4.8. DLS measurements for the diffusion coefficient of the hybridized and non-hybridized sequences  $A_5G_7$ -*b*-PB<sub>2000</sub> and  $G_{12}$ -*b*-PB<sub>2000</sub>.

The scattering intensities in the measurements were always kept in the range of 80-500 kHz, but differently from the results obtained with the non-hybridized oligonucleotides, the polydispersity indices were in the range of 0,3 to 0,45, indicating that the samples became more polydisperse after hybridization. This is in agreement with what was suspected in the analysis of SEC.

The correlation curves obtained in the DLS analyses of the hybridized polymer-modified oligonucleotides did not show any artifacts or unusual behavior, being only slower than what was observed for the non-hybridized copolymers, which indicates no structural change.

It is interesting to observe that the two linear regressions shown in figure 4.5 seem to converge at the limit of  $C \rightarrow 0$ . This means that the diffusion coefficients  $D_0$  of both hybridized copolymers would be similar. Hybridization of self-assembled polymer-modified nucleotide sequences of different compositions yields self-assembled structures with approximately the same  $R_h$  (table 4.1).

Copolymer	$D_0$ ( $m^2/s$ )	$R_h$ (nm)	$\Delta R_h$ (nm)	Error (%)
$G_{12}$ - <i>b</i> -PB <sub>2000</sub> + C <sub>12</sub>	$4,79 \cdot 10^{-13}$	447	140	32
$A_5G_7$ - <i>b</i> -PB <sub>2000</sub> + C <sub>7T5</sub>	$4,95 \cdot 10^{-13}$	432	156	36

Table 4.5. DLS results for the self-assembled structures of the hybridized oligonucleotide-based block copolymers.

One can observe that the modification in the dimensions of the self-assembled structures upon hybridization is significant when compared with the size of non-hybridized self-assembled oligonucleotide-based copolymers (92% for  $G_{12}$ -*b*-PB<sub>2000</sub> and 34% for  $A_5G_7$ -*b*-PB<sub>2000</sub>). This could be explained by the increase in excluded volume due to the hybridization process, inducing an increase in the dimensions of the self-assemblies, the change of the hydrophobic to hydrophilic balance and the stiffening of the nucleotide shell.

The data obtained also confirm the hypothesis that the polydispersity of the sample is higher than that of the non-hybridized self-assembled copolymer, given that the error in the hydrodynamic radius is much bigger than reported prior to hybridization. This higher polydispersity of the samples is probably an effect of a non-homogeneous hybridization process among the self-assembled structures.

The reason for the similarity in hydrodynamic radius observed between both hybridized polymer-modified oligonucleotides, though not clear at first, is the very formation of the double helix by the oligonucleotide.

The size of the non-hybridized self-assembled structures presents a dependence on the composition of the sequence composing the oligonucleotide-based copolymer, as previously observed (section 3.3.1: Size Determination). This dependence arises from differences in the conformation and excluded volume of each individual oligonucleotide sequence.

The formation of the double helix, however, eliminates this dependence, since upon the H-bonding of the nucleic bases the helix achieves a standard conformation with constant width (2,2-2,6 nm<sup>14</sup>). This leads also to a constant excluded volume of the helix, resulting in similar values for the hydrodynamic radius of the self-assembled nucleotide based copolymers, regardless of the nucleotide sequence composition.

## 4.2. Preliminary Biological Assays

Once determined that the oligonucleotide sequences within the self-assembled structures retain their ability to undergo hybridization, in order to develop applications for biological systems it is necessary to study whether the polymer-modified oligonucleotides induce any toxic effects. Although poly(butadiene) is a non-

FDA approved material for use *in vivo*<sup>15</sup>, several *in vitro* studies have been reported using PB as component of drug delivery carrier systems<sup>16,17</sup>.

#### 4.2.1. Cytotoxicity studies

In order to assess the cytotoxicity of the oligonucleotide-based copolymer systems, three different cells lines were selected: BHK (baby hamster kidney), HEK (human embryonic kidney) and SaSO2 (human osteosarcoma). These cell lines were chosen to perform representative assays due to their relative easiness of culture and widely disseminated use in cell biology, such as transfection and cancer therapy<sup>18,19,20</sup>.

Cells were grown in 6-well plates using McCoy's 5A modified medium (Sigma-Aldrich) until confluence (approximately 24 h). They were detached from the wells by using a Trypsin-EDTA solution and stained with Trypan blue, a common dead/alive dye that permeates the membrane of dead cells, turning them blue<sup>3</sup>.

The cytotoxicity of the polymer-modified oligonucleotides was determined by a viability quantitative assay. In this assay, one calculates the relation between the total number of cells and the number of non-viable ones in a control sample (without the material to be studied) and a test sample (with the material). The comparison between the two values will provide a good indication of the cytotoxicity of the tested material<sup>3</sup>.

The polymer-modified oligonucleotides chosen to be used in these experiments were A<sub>5</sub>G<sub>7</sub>-*b*-PB<sub>2000</sub> (data not shown) and G<sub>12</sub>-*b*-PB<sub>2000</sub>. The solutions of the copolymers were prepared from the original normalized concentration in the dilutions (v/v) of 1:10, 1:50, 1:100 and 1:1000. The experiments were repeated three times in order to evaluate the accuracy and reproducibility of the assay.

The result of one of the series of experiments performed with the nucleotide-base copolymers is shown (table 4.2). The error was calculated by the standard error obtained from the three repetitions of the experiment.

N	HEK with G12-b-PB2000				HEK Control			
	Total (10 <sup>6</sup> cells/mL)	Viable (10 <sup>6</sup> cells/mL)	Non-viable (10 <sup>6</sup> cells/mL)	% non-viable	Total (10 <sup>6</sup> cells/mL)	Viable (10 <sup>6</sup> cells/mL)	Non-viable (10 <sup>6</sup> cells/mL)	% non-viable
1	1,77	1,7	0,07	3,955	1,6	1,57	0,03	1,875
2	1,75	1,73	0,02	1,143	1,55	1,51	0,04	2,581
3	1,79	1,75	0,04	2,235	1,75	1,72	0,03	1,714
<b>Average</b>	<b>1,770</b>	<b>1,727</b>	<b>0,043</b>	<b>2,444</b>	<b>1,633</b>	<b>1,600</b>	<b>0,033</b>	<b>2,057</b>
<b>Error</b>	<b>0,020</b>	<b>0,025</b>	<b>0,025</b>	<b>1,418</b>	<b>0,104</b>	<b>0,108</b>	<b>0,006</b>	<b>0,461</b>

Table 4.6. Cytotoxicity studies performed for a 1:50 solution of G<sub>12</sub>-b-PB<sub>2000</sub> with the HEK cell line.

The complete results of the experiments performed with G<sub>12</sub>-b-PB<sub>2000</sub> may be observed in figure 4.7.

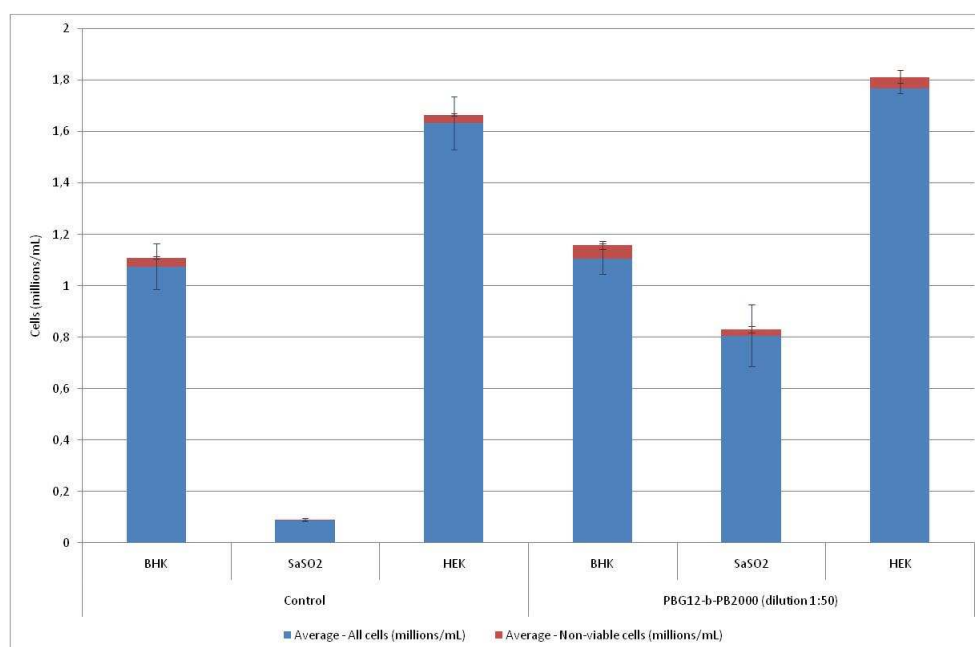


Figure 4.9. Complete cytotoxicity assays performed for a 1:50 solution of the copolymer G<sub>12</sub>-b-PB<sub>2000</sub> (blue: viable cells and red: non-viable cells).

One can conclude that these experiments evidenced very low cytotoxicity of G<sub>12</sub>-b-PB<sub>2000</sub>, since no visible increase in the percentage of non-viable cells can be perceived. The results of the experiments with A<sub>5</sub>G<sub>7</sub>-b-PB<sub>2000</sub> lead to the same conclusion.

The cells incubated with the nucleotide-based copolymers were imaged with a Zeiss LSM510 microscope (figure 4.8). The morphological characteristics of the cells seemed to be well preserved after incubation, which further supported the low toxicity of the polymer-modified oligonucleotides.

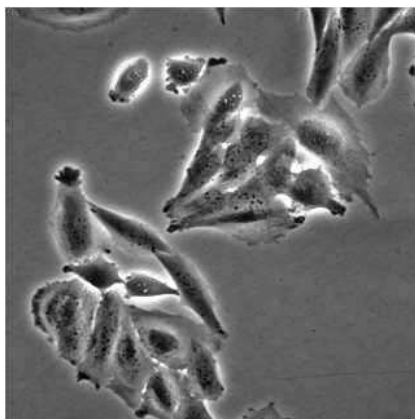


Figure 4.10. Spreading SaSO2 cells incubated with a 1:50 solution of  $G_{12}$ - $b$ -PB<sub>2000</sub>.

#### 4.2.2. Internalization studies

Despite the fact that polymer-oligonucleotides did not induce cell death in the samples studied, we could not access whether the self-assembled structures were internalized by the cells, which is an important feature if one wishes to develop a carrier system. In order to resolve this point, further studies with macrophages were performed to determine if the polymer-modified oligonucleotides could be uptaken. Macrophages were chosen due to their high internalization ability, which would facilitate observation of the process.

The self-assembled structures were labeled with the DNA chelating agent Syto9<sup>®</sup> (Invitrogen). After labeling, the polymer-modified oligonucleotide solution was incubated with the macrophages for 1h. A negative control sample was prepared, in which Syto9<sup>®</sup> was added directly to the macrophages, without the nucleotide-based copolymer, and incubated for one hour.

A third sample was prepared, in which the nucleotide-based copolymer was labeled with Syto9<sup>®</sup> and the macrophages were labeled with another DNA chelating agent, Hoescht (Invitrogen). Once again, after adding the copolymer solution to the macrophages, the sample was incubated, but this time for 30 min. The samples were then transferred to a 6-well plate and observed with a Zeiss LSM510 microscope (figure 4.9).



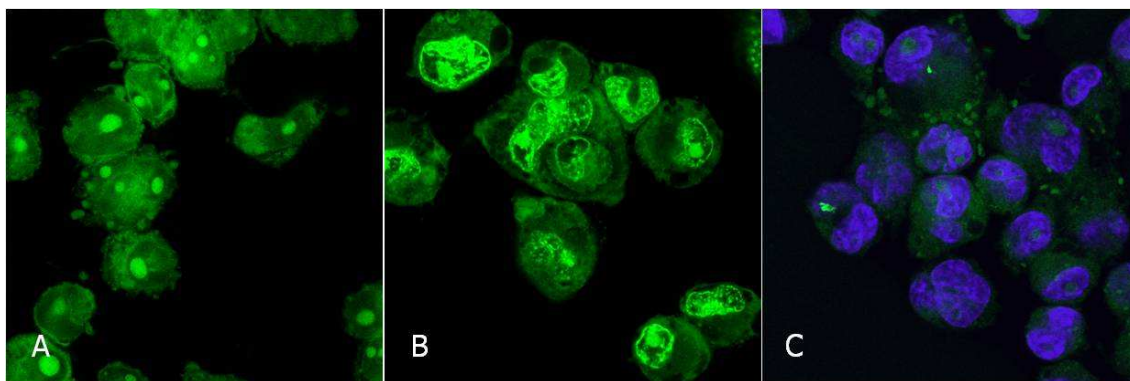


Figure 4.11. Macrophage internalization assays imaged by CLSM: A)  $C_{12}$ - $b$ - $PB_{2000}$  labeled with Syto9<sup>®</sup>, B) macrophages labeled with Syto9<sup>®</sup> and C)  $C_{12}$ - $b$ - $PB_{2000}$  labeled with Syto9<sup>®</sup> + macrophages labeled with Hoescht.

One can observe in figure 4.9-A that after incubation some vesicular structures, which are brighter than the other regions of the cell, can be observed inside the macrophages. These structures are probably the result of the internalization process, either phagocytosis or recognition-driven uptake<sup>21</sup>, of the self-assembled structures, what explains the locally higher concentration of Syto9<sup>®</sup>.

The sample in which only the Syto9<sup>®</sup> was added (figure 4.9-B), one can observe a completely different labeling pattern, as the DNA in the nuclei of the macrophages are chelated by the dye. This result leads to the hypothesis that, upon uptake, the polymer-modified nucleotides remain inside the endosomes/lysosomes, along with the dye.

The third assay (figure 4.9-C) was performed in a shorter timeframe in order to observe how long until the internalization process would occur. One can observe that, though some structures are already present in the cytoplasm, the internalization process was still taking place, as most of the lysosomes can be observed close to the outer membrane of the cell. The use of two dyes allows the observation that none of the Syto9<sup>®</sup> penetrates the nuclear membrane, remaining bound to the nucleotide-based copolymer.

These results prove that internalization of the self-assembled structures occurs, although at this point it is not possible to determine through which mechanism this process occurs. Further experiments are still necessary in order to clarify this internalization process.

### 4.3. References

39. Watson, J.; Crick, F. Molecular Structure of Nucleic Acids – A Structure for Deoxyribose Nucleic Acid *Nature*, **1953**, *171*, 737–738..
40. *Protocols for Oligonucleotides and Analogs, synthesis and properties*; Agrawal, S., Ed.; Humana Press Inc.: Totowa, NJ, 1993; Volume 20.
41. Sambrook, J.; MacCallum, P. *Molecular Cloning, A Laboratory Manual*, 3<sup>rd</sup> Edition; Cold Spring Harbor Laboratory Press: New York, NY, USA, 2001.
42. Solomons, T.W.G.; Fryhle, C.B. *Organic Chemistry*, 7<sup>th</sup> Edition; John Wiley and Sons, Inc.: New York, NY, USA, 2000.
43. Razumovitch, J.; Meier, W.; Vebert-Nardin, C. A microcontact printing approach to the immobilization of oligonucleotide brushes. *Biophys. Chem.* **2009**, *139*, 70-74.
44. Maruyama, T.; Hosogi, T.; Goto, M. Sequence-selective extraction of single-stranded DNA using DNA-functionalized reverse micelles. *Chem. Commun.* **2007**, 4450-4452.
45. Yoshikawa, K. Single Macromolecules: Hierarchic Thermodynamics, Irreversibility and Biological Function. *J. Biol. Phys.* **2005**, *31*, 243-248.
46. Lecolley, F.; Tao, L.; Mantovani, G.; Durkin, I.; Lautru, S.; Haddleton, D.M. A new approach to bioconjugates for proteins and peptides (pegylation) utilising living radical polymerization. *Chem. Commun.* **2004**, 2026-2027.
47. Halperin, A.; Buhot, A.; Zhulina, E. B., Brush effects on DNA chips: thermodynamics, kinetics, and design guidelines. *Biophys. J.* **2005**, *89*, 796-811.
48. Brown, P.O.; Botstein, D. Exploring the new world of the genome with DNA microarrays. *Nat. Genet.* **1999**, *21*, 33-37.
49. Dickerson, R.E.; Drew, H.R.; Conner, B.N.; Wing, R.M.; Fratini, A.V.; Kopka, M.L. The anatomy of A-, B-, and Z-DNA. *Science* **1982**, *216*, 475-485.
50. Nardin, C.; Hirt, T.; Leukel J.; Meier, W. Polymerized ABA triblock copolymer vesicles. *Langmuir*, **2000**, *16*, 1035-1041.
51. Razumovitch, J.; de França, K.; Kehl, F.; Wiki, M.; Meier, W.; Vebert, C. Optimal Hybridization Efficiency of Surface Tethered Oligonucleotides: a comparative quantification with the quartz crystal microbalance and the wavelength interrogated optical sensor. *Biomacromolecules* 2009, *accepted*.

52. Mandelkern, M.; Elias, J.; Eden, D.; Crothers, D. The dimensions of DNA in solution. *J. Mol. Biol.* **1981**, *152*, 153-161.
53. FDA website: <http://www.fda.gov/default.htm>, accessed on: 23 April 2009.
54. Li, S.; Byrne, B.; Welsh, J.; Palmer, A.F. Self-Assembled Poly(butadiene)-b-Poly(ethylene oxide) Polymersomes as Paclitaxel Carriers. *Biotechnol. Prog.* **2007**, *23*, 278-285.
55. Kima, Y.; Tewaria, M.; Pajerowskia, J.D.; Caia, S.; Sena, S.; Williams, J.; Sirsi, S.; Lutz, G.; Discher, D.E. Polymersome delivery of siRNA and antisense oligonucleotides. *J. Controlled Release* **2009**, *134*, 132-140.
56. Zheng, H.; Tian, H.; Jin, Y.; Wu, J.; Shang, Y.; Yin, S.; Liu, X.; Xie, Q. Development of a hamster kidney cell line expressing stably T7 RNA polymerase using retroviral gene transfer technology for efficient rescue of infectious foot-and-mouth disease virus. *J. Virol. Methods* **2009**, *156*, 129-37.
57. Thomas, P.; Smart, T.G. HEK293 cell line: a vehicle for the expression of recombinant proteins. *J. Pharmacol. Toxicol. Methods* **2005**, *51*, 187-200.
58. Zheng, X.; Rao, X.M.; Snodgrass, C.L.; McMasters, K.M.; Zhou, H.S. Selective replication of E1B55K-deleted adenoviruses depends on enhanced E1A expression in cancer cells. *Cancer Gene Ther.* **2006**, *13*, 572-83.
59. Broz, P.; Benito, S.M.; Saw, C.; Burger, P.; Heider, H.; Pfisterer, M.; Marsch, S.; Meier, W.; Hunziker, P. Cell targeting by a generic receptor-targeted polymer nanocontainer platform. *J. Control. Release*, **2005**, *102*, 475-488.

## Chapter 5: Conclusion and Outlook

The main purpose of the doctoral research work here presented was to synthesize oligonucleotide-based copolymer systems and study their self-assembly in dilute aqueous solutions, analyzing which elements or variables would affect the self-assembly mechanism. Further than that, in order to evaluate whether the polymer-modified oligonucleotide would be able to trigger specific recognition in biological systems after polymer modification and upon self-assembly, preliminary analysis regarding the hybridization ability of these copolymers in solution were performed.

The oligonucleotide-based copolymers were successfully synthesized through two different synthetic pathways: solid phase chemistry and heterogeneous biphasic chemistry. These two methodologies were developed taking in consideration the chemical and physical characteristics of the oligonucleotide and the polymer involved in the synthesis. The oligonucleotide sequences used were 12-nucleotide long and the hydrophobic polymer chosen was poly(butadiene), due to its low glass transition temperature and cross-linkability.

The self-assembly of these nucleotide-based copolymers was studied in different dilute aqueous solutions, namely pure doubly distilled water, phosphate buffer saline, PBS and tris-EDTA with 50 mM of NaCl added, TE+NaCl buffers. It was proved that the polymer-modified oligonucleotides self-assemble into vesicles.

Due to the fact that oligonucleotides behave as charged polymers in solution, the morphology and size of the vesicular structures were directly dependent on the ionic strength of the solution. In pure water, small structures were observed in coexistence with large, more complex ones. In the buffers, the self-assembled structures presented a more homogeneous size distribution.

It was also observed that, when coupled to a PB block of the same length, the size of the self-assembled structures were not only dependant on the number of bases in the oligonucleotides strands, but also on the actual sequence of bases composing the oligonucleotide.

The mechanical reinforcement of the self-assembled structures by cross-linking the PB was also studied, showing that the stability of the vesicles to osmotic stress was increased after the process.

Configurational analyses were performed and determined that the oligonucleotide sequences within the self-assembled structures did not suffer any configurational changes due to the synthetic and self-assembly processes of the polymer-modified oligonucleotides.

Preliminary hybridization studies were also performed and showed that the strands within the vesicular shell retained their ability to form double helices by base pairing. Hybridization within self-assembled structures led to a higher polydispersity degree than what was observed prior to hybridization. This result is probably a consequence of the high density of oligonucleotides on the surface of the vesicles, leading to incomplete and irregular hybridization of the strands.

Biological essays were performed in order to assess the cytotoxicity and internalization ability of the system. The cell viability tests showed no toxic effect of the polymer-modified oligonucleotides on the cell lines studied in the concentration range investigated. Internalization studies showed that upon uptake by immune cells the oligonucleotide-based copolymer remains within the endosomes.

The results obtained in this research work show that oligonucleotide-based copolymers are very promising for actual application in drug delivery and sensing technologies based on hybridization, such as DNA chips.

Bearing in mind these conclusions, the outlook for utilization of these oligonucleotide-based copolymers is quite large.

For instance, the use of oligonucleotide sequences with a different number of bases and different hydrophobic polymer blocks may lead to the self-assembly of these oligonucleotide-based copolymers into various morphologies, and by fine tuning of the sequence composition one can control the size of the structures obtained in the self-assembly process.

In order to improve the degree of hybridization of the sequences within the self-assembled structures, the base-pairing process onto densely packed surface needs to be better understood. There are already studies being performed in order to understand this process, but not within the scope of this project.

Encapsulation assays to determine the loading capability of these polymer-modified oligonucleotide self-assembled structures and the permeability of the membrane would be very useful in order to develop this system for applications in drug delivery and gene therapy.

Biological assays to determine the biocompatibility of these oligonucleotide-based systems should be performed in order to determine which sequences are able to undergo specific recognition by cells and to understand the uptake mechanism through which the self-assembled structures are internalized.

In order to reduce the cost of these oligonucleotide-based systems, possibly one of the biggest problems to develop commercial applications of these materials, one can think about the use of hybrid systems, in which the polymer-modified oligonucleotides would be used as an additive to other, more inexpensive copolymer, such as poly(ethylene oxide), PEG based copolymers. This sort of system would combine the specific recognition ability of the oligonucleotides with the stealth properties of PEG.

Many other applications can and will be developed for polymer-modified oligonucleotide systems in the future, but considering the scope of this project, we believe that we were able to contribute towards the utilization of biologically active self-assembled interfaces for use in different scientific fields.

## Chapter 6: Materials and Methods

The following materials and methods were used in order to support the performance of these research studies.

**FT-IR analyses.** Sample analysis was performed on solid phase using a Shimadzu FTIR 8400 equipment (Shimadzu Scientific Equipments). The measurements were performed using either air or poly(butadiene) to set the background prior to analysis.

**<sup>1</sup>H-NMR analyses.** The samples for <sup>1</sup>H-NMR analyses were prepared by direct dilution of the lyophilized nucleotide-based copolymers in 0,7 mL of the appropriate solvent (CDCl<sub>3</sub>, D<sub>2</sub>O, 5% D<sub>2</sub>O/H<sub>2</sub>O). Concentration of the solutions was in the range of 100 nM to 1 μM. All NMR experiments were performed at 22 °C on a Bruker DPX-400 NMR spectrometer, equipped with a QNP probehead. Chemical shifts were referenced to residual solvent peaks and the temperature was calibrated using a methanol sample.

**GPC analyses.** GPC samples were prepared by dissolution of the polymer/copolymer in chloroform to a concentration of 2 mg.mL<sup>-1</sup>. After dissolution, the samples were left overnight for complete solubilization of the material. Prior to injection, the samples were filtered through hydrophobic 0,2 μm filters. GPC analysis of polymer molecular weights was performed using Agilent Technologies GPC instrument. All molecular weights were corrected according to poly(butadiene) standards. A refractive index detector was employed for sample detection. Chloroform was used as the elution solvent.

**ESI-MS analyses.** Small amounts of the lyophilized oligonucleotide-based block copolymer sample in TE+NaCl buffer were dissolved in 100 μL methanol (MeOH). 1:100 dilutions of the samples into 0.1% triethylamine (NEt<sub>3</sub>) were prepared. Electrospray ionization of the polymer-modified oligonucleotides samples were performed in negative mode, with multiple charged peaks for molecules of the expected size expected.

**DLS analyses.** DLS samples were prepared by dissolution of the oligonucleotide-based block copolymer solution obtained after SEC. These concentrations were normalized based on that first solution. Each of these solutions had a minimum volume of 1 mL. All the samples were centrifuged at 4000 rpm for 10-15 min prior to analysis to settle any dust particles or eventual aggregates of material that could interfere in the result of the measurements. The self-assembled polymer-modified oligonucleotides were analyzed by DLS using a goniometer equipped with a 632 nm He-Ne laser (ALV, Germany) at 293 K (for PBS solutions) or 300 K (for TE+NaCl solutions). The scattering angles used were between 30° and 150°, with a correlation time of 300 s. The DLS correlation data was analyzed via cumulant or non-linear ( $g^2(t)$ ) fit model using the ALV-Correlator Software (ALV, Germany).

**AFM analyses.** Analyses were performed using a Nanoscope IIIa D3000 atomic force microscope, from Digital Instruments. Tapping mode. silicon cantilever: phosphorous doped Si, f:272-318kHz, K=20-80N/m from Veeco.

**TEM analyses.** TEM grids were prepared by pre-coating 300 mesh copper grids with a layer of parlodium n-butyl acetate and a layer of carbon. The polymer-modified oligonucleotide solutions were prepared for TEM imaging by diluting the solutions from the DLS measurements with PBS or TE+NaCl buffer, depending on the solution used for the SEC of the nucleotide-based copolymer. The final concentration was in the range of 0,01-0,001 (based on the normalized concentration after SEC). The TEM grids were submitted to a voltage of 75-80 V under vacuum, in order to allow deposition of the self-assembled structures. The solutions were deposited by letting 0,005 cm<sup>3</sup> of solution rest for 60 s on the grid and removing the excess of solution by dabbing with a Kim wipe leaving the self-assembled nucleotide-based copolymers onto the film. No staining of the samples was performed. The self-assembled structures were imaged using a FEI (Philips) Morgani 268D (figure 6.1) with an accelerating voltage of 80 kV (max 100 kV).





Figure 6.12. TEM FEI (Philips) Morgani 268D microscope.

**SEM analyses.** The sample preparation for SEM was performed using the same copper grids used for TEM analyses. After deposition of the self-assembled structures, the grid was washed with bi-distilled water by dipping the surface of the grid. The excess water was removed by dabbing with a Kim wipe. Prior to analysis, the samples were spur coated with a 20 nm gold layer using a Bal-Tec MED 020 Coating System. Imaging was performed with a Philips XL 30 ESEM microscope (figure 6.2), which operates at water vapour pressures of 10 Torr or higher with a dedicated gaseous secondary electron detector, GSED that allows true secondary electron imaging at full SEM resolution.



Figure 6.13. Philips XL 30 ESEM microscope.

**CLSM analyses.** CLSM studies were performed with a Zeiss light scanning microscope (LSM) 510 Meta (figure 6.3), an inverted confocal light microscope which is equipped with an ultraviolet (405 nm), an Argon ion (458 nm, 477 nm, 488 nm, 514 nm), and two Helium Neon lasers (543 and 633 nm). All the lasers in the laser module are passed through an acousto-optical tunable filter which enables

continuous adjustment of the level of transmission and are then guided through an optical fiber cable to the scan head enabling frame scanning. The light passing through the objective in an epi-illumination configuration is then reflected at the specimen and the reflected light is collected with the same objective and passes through the confocal pinhole before it hits a photomultiplier tube (PMT). This microscope is also equipped with an array-PMT detector (Meta detector) which enables acquisition of whole spectra. The microscope has infinity corrected optics and is equipped with the following objectives: a standard 15x air low numerical aperture (NA) objective, a 25x immersion objective, a 40x C-Apochromat 1.2 NA water-immersion objective corrected for chromatic aberrations, a 63x C-Apochromat 1.2 NA water-immersion objective, and a 100x Plan-Apochromat 1.4 NA oil-immersion objective. The motorized Axiovert 200M microscope as well as image acquisition and subsequent data treatment is completely controlled by the ZEISS advanced imaging (AIM) software.

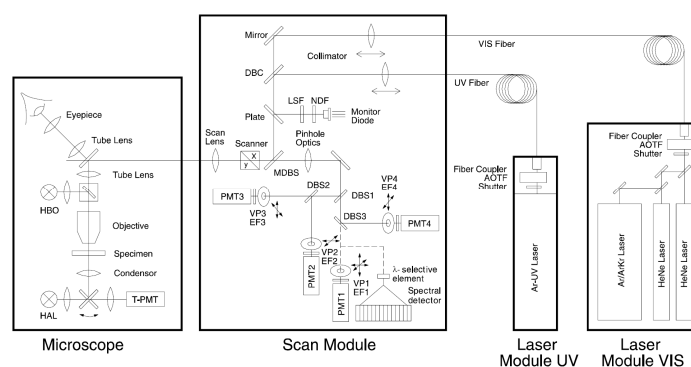


Figure 6.14. Schematic optical path of the ZEISS LSM 510 Meta microscope.

## CURRICULUM VITAE

### FRANCISCO JOSÉ TEIXEIRA JR.

Grienstrasse, 41  
4055 - Basel  
Switzerland  
+41 61 267 3843 (work)  
+41 78 673 7220 (mobile)  
+41 61 534 0621 (home)  
Francisco.Teixeira@unibas.ch



#### PROFILE

---

- ✓ PhD in Chemistry with focus on synthesis and characterization;
- ✓ Chemical Engineering degree with emphasis on thermoplastic elastomers;
- ✓ Industrial experience in synthesis and physico-chemical characterization;
- ✓ Industrial experience in optimization of commercial processes;
- ✓ Knowledge of quality improvement and maintenance programs;
- ✓ Hard-working and motivated.

#### PROFESSIONAL ACTIVITIES AND TRAINING

---

- Since 04/09 **Molecular Diversity Preservation International (MDPI) – Basel, Switzerland**  
Managing Editor:  
✓ Responsible for the publication of several scientific journals.
- 09/05 - 03/09 **Chemistry Department, University of Basel – Basel, Switzerland**  
PhD Research  
✓ Synthesis and Characterization of Polymer Modified Oligonucleotides
- 09/04 - 08/05 **Novartis Pharma AG – Basel, Switzerland**  
Trainee in Pharmaceutical Research in a Medicinal Organic Chemistry Laboratory:  
✓ Planning and preparation of small scale organic and organometallic synthesis;  
✓ Interpretation of analytics (NMR, MS, LC/MS).
- 02/04 - 08/04 **Petroflex Indústria e Comércio S.A. – Cabo de Santo Agostinho, PE, Brazil**  
Trainee in Chemical Engineering:  
✓ Assistance in the Optimization in the Production of Thermoplastic Rubbers (TR);  
✓ Accompaniment of the Production of Synthetic Rubbers and the Supply of Water and Steam to the Industrial Plant;

- ✓ Participation in Quality Programs such as 5S and 6 $\delta$ ;
- ✓ Participation in the implementation of Balance Score Card (BSC) Quality Program.

#### ACADEMIC FORMATION

---

09/05 - 05/09 **PhD in Chemistry**

Chemistry Department, University of Basel – Basel, Switzerland  
PhD Student under the supervision of Dr. Corinne Vebert-Nardin

- ✓ Doctoral Thesis: *“Polymer-Modified Oligonucleotide Sequences: Towards Biologically Active Self-Assembled Interfaces”*

03/99 - 08/04 **Chemical Engineering**

Universidade Federal de Pernambuco, UFPE – Recife, Brazil

- ✓ Diploma Thesis: *“Optimization in the Quality of the Variables Color and Gel in the Production of Linear Thermoplastic Rubbers”*

#### OTHER EXPERIENCES

---

- 2008 Physical-chemistry I Lecturing assistant – University of Basel – Basel, Switzerland
- 2006 – 2007 Physical-chemistry Praktikum Lecturing Assistant – University of Basel – Basel, Switzerland
- 2001 – 2004 Organic Chemistry Lecturing Assistant – UFPE – Recife, PE, Brazil
- 2002 - 2003 Undergraduate Research Scholarship – *“Technology of Aromatics & Hydrogen Production from Natural Gas”* from ANP/PRH-28 (National Petroleum Agency/Human Resources Program - 28) – UFPE, Recife, PE, Brazil
- 2000 - 2001 Undergraduate Research Scholarship – *“Simulation of an Illumination Optical Fiber Extrusion Molding Process”* from Pibic/FACEPE-CNPq (Brazilian National Research Agency/Ministry for Science and Technology) – UFPE, Recife, PE, Brazil

#### PUBLICATIONS

---

1. Teixeira Jr., F.; Rigler, P.; Vebert-Nardin, C. Nucleo-copolymers: oligonucleotide-based amphiphilic diblock copolymers. *Chem. Commun.* **2007**, 1130-1132.
2. Wigglesworth, T.J.; Teixeira Jr., F.; Axthelm, F.; Sara Eisler, S.; Noemi S. Csaba, N.S.; Hans P. Merkle, H.P.; Wolfgang Meier, W.; Diederich, F. Dendronised block copolymers as potential vectors for gene transfection. *Org. Biomol. Chem.* **2008**, 6, 1905-1911.
3. Cottenye, N.; Teixeira Jr., F.; Ponche, A.; Reiter, G.; Anselme, K.; Meier, W.; Ploux, L.; Vebert-Nardin, C. Oligonucleotide nanostructured surfaces: effect on *Escherichia coli* curli expression. *Macromol. Biosci.* **2008**, 8, 1161-1172.

## Vitae

4. Teixeira Jr., F; Nussbaumer, M.; Syga, M.-I.; Nosov, S.; Müller, A.H.E.; Vebert-Nardin, C. Polymer-modified oligonucleotides: synthesis and characterization of biologically active self-assembled interfaces. *In preparation*.

---

**LANGUAGES**

---

1. Portuguese – mother language
2. English – fluent
3. German – intermediary
4. Spanish – intermediary

---

**PERSONAL INFORMATION**

---

- ✓ Brazilian, 28 years old, married;
- ✓ Swiss Permit B;
- ✓ Interest in sports, music, cinema and traveling.

---

**PERSONAL REFERENCES**

---

**Dr. Corinne Vebert-Nardin**

University of Basel  
Chemistry Department  
Phone Number: +41 61 267 3843  
E-mail: Corinne.Vebert@unibas.ch

**Prof. Dr. Wolfgang Meier**

University of Basel  
Chemistry Department  
Phone Number: +41 61 267 3802  
E-mail: Wolfgang.Meier@unibas.ch

**Dr. Rudolf Waelchli**

Novartis Pharma AG  
Phone Number: +41 61 324 6473  
E-mail: Rudolf.Waelchli@novartis.com